Criterion of Vehicle Instability in Floodwaters: Past, Present and Future

Shah*, Syed Muzzamil Hussain; Universiti Teknologi PETRONAS, Civil and Environmental Engineering

Mustaffa, Zahiraniza; Universiti Teknologi PETRONAS

Martinez-Gomariz, Eduardo; Flumen Research Institute (Technical University of Catalonia)

Kim, Do Kyun ; Universiti Teknologi PETRONAS

Yusof, Khamaruzaman ; Universiti Teknologi PETRONAS Faculty of Engineering, Civil and Environmental Engineering

*Corresponding author

ABSTRACT

The stability of vehicles exposed to floodwaters on the roads should not be taken for granted, especially in floodplain areas. When a vehicle in floodwaters becomes unstable, it tends to become buoyant and, eventually, is washed away, putting occupants in extreme danger. Therefore, the characteristics of vehicle instability in floodwaters should be critically understood to prepare safety guidelines. This paper attempts to summarize different vehicle stability studies, which focused on parked vehicles for a range of flood depths, through experimental and theoretical analysis (1967-1993). However, modern vehicle designs mean there are different values for the stability limits under partial or full submergence with different braking conditions, orientations and ground slopes (2010-2017). Since all the reported studies are about static vehicles, this paper attempts to address, for the very first time, vehicles in motion and endangered by floodwaters. As such, the governing effect of incipient velocity for a partially submerged, non-stationary vehicle will be presented, under the consideration of two new parameters, namely rolling friction and driving force.

Keywords: vehicle instability, floodwater, non-stationary vehicles.

1.0 INTRODUCTION

The probability of flood occurrence has increased due to considerable meteorological changes, which has also increased the risk of vehicle instability in floodwaters [1]. The vehicle may have very undesirable dynamics under certain conditions [2] causing it to become unbalanced either by floating, when the water depth is high and flow velocity is low, or by losing the frictional resistance between the tires and the ground surface (sliding) when the flow velocity is high and the water depth is low [1]. In this way, the vehicles might be considered massive debris being washed away by the flood, which could compromise pedestrian safety and generate significant economic damages [3]. A clear illustration of these damages is the heavy downpour which caused a devastating flash flood in low-lying areas near Sungai Pinang and Sungai Air Itam in Penang, Malaysia on 15th September 2017, as shown in Figure 1. The Malaysian Department of Irrigation and

Drainage (DID) reported that both rivers reached the highest levels recorded, i.e., 3.2 m (Sungai Pinang) and 7.3 m (Sungai Air Itam). The rainfall recorded at Sungai Pinang and Sungai Air Itam station was 198 mm and 120.5 mm, respectively. There was massive traffic gridlock on the roads because vehicles were submerged in floodwaters at depths between 0.1 m to 0.6 m [4].

Roads are reported to be the first assets affected by floods [5]. It represents a major threat to both passengers and bystanders, including injuries or deaths. It further damages the infrastructure and blocks hydraulic structures [6]. Almost half of the people trapped by floods on roads are car passengers. Improper drainage along road crossings interrupts floodwater flows, leading to variations in the states and characteristics of the flowing water. They further damage the channel structure; thus, the chances of threats around such structures would increase, which usually ends up as a serious traffic hazard [7]. The increasing number of vehicles in many cities also causes traffic disruption during such events, which is usually overlooked, and is regarded as an indirect impact of flooding [8].

Hazards related to vehicles exposed to floodwater are based on their stability threshold, which is assessed from hydraulic variables, *i.e.* water depth and velocity [9], [10] and [11]. A vehicle's stability will be compromised when the hydraulic variables exceed a certain limit, similar to the stability thresholds of pedestrians exposed to floodwater flows [12], [13] and [14]. In case of vehicles, characteristics like weight, ground clearance, sealing capacity and design determine the stability level [3]. Existing vehicle safety design guidelines are based on the product of flow depth and velocity. These values are obtained during experimental investigations and the theoretical analyses of stationary vehicles in late 1960s, early 1970s and early 1990s. However, today's vehicles are different from past designs, and new improvements have been taken into consideration; therefore, the results of these earlier studies may no longer apply to contemporary vehicles [15]. Although public safety is the primary aim of any flood risk management strategy, studies of vehicles' instability under water flow are sparse, and existing hazard criteria are unreliable for examining urban flood scale [16].

This paper incorporates the most comprehensive examination of vehicles exposed to floodwaters to date. Further, it interrogates the relationships between the past and current empirical as well as theoretical approaches describing the limits of stability in terms of flow depth and velocity for the stationary model vehicles. A static vehicle is affected by several hydrodynamic forces, namely buoyancy, lift, drag and frictional force as it gets in contacts to floodwaters. Based on the dominancy of the given forces, it would further lead to the possibility of instability failure mechanism, *i.e.* sliding or floating. Conversely, when a non-stationary vehicle attempts to cross a flat flooded street when the direction of flow is perpendicular to the vehicle movement, it is not only affected by the above-mentioned forces, but also by the driving force caused by the vehicle engine and the rolling friction of tires. The driving force mechanics, however, are still not well understood when a vehicle enters floodwater. Moreover, the contribution of rolling friction caused by tires' rotation should not be taken for granted. Herein a novel approach to predict the incipient velocities for the moving vehicles under partial submergence, where the state of the flow remains sub-critical, has been introduced for the first time. This is essential for updating the current safety design guidelines.

2.0 THEORITICAL BACKGROUND

2.1 Hydrodynamic Forces

Moving water, particularly floodwaters, creates hydrodynamic forces to move a vehicle located in a floodplain, as shown in Figure 2. Understanding of the relevant forces involved is necessary to characterize stability thresholds of vehicles in floodwaters through the relationships of friction, gravitational, buoyancy, lift, and drag forces.

Frictional resistance is basically the relative motion of two solid objects, which is proportional to the surface roughness and the normal force pressing the surfaces together. The frictional force is presumed to be proportional to the coefficient of friction. Therefore, when an object is at rest, it requires effort to move because there is some frictional force acting between the object and the floor. This friction holds the object in place and prevents changing the state of rest. This is called static friction. Once the object starts to slide, the static friction becomes zero. However, there is still some resistive force, called sliding friction. Rolling friction is the resistive force that slows a body which rolls on a surface such as balls, wheels etc. The rolling friction is smaller than sliding friction because the interlocking between the two surfaces is minimum in this case [17]. Frictional force varies depending on the state of brakes being applied. However, once the vehicle is lifted off from the surface, the frictional force becomes zero. The general formula for the friction force, F_R can be expressed as:

$$F_R = \mu F_G \tag{1}$$

where, μ is the coefficient of friction and F_G is the net weight of the vehicle [18]. The friction coefficient is simply a material property that relates to the two bodies involved and can be best estimated experimentally [19]. On the other hand, the net weight of the vehicle F_G, can be determined by deducting the buoyancy force from the total weight of the car and can be expressed as:

$$F_G = F_g - F_B \tag{2}$$

where, F_g is the total weight of the vehicle and F_B is the buoyancy force [20].

When a body is submerged in fluid, the resultant force acting on the body is formed in an upward vertical direction. This force, which is also known as the buoyancy force, is generated because of the pressure which increases with depth. These pressure forces acting from below are larger than the pressure forces acting from above. Therefore, the buoyancy force has a magnitude equal to the weight of the fluid displaced by the body and is directed vertically upward. This phenomenon is commonly referred to as Archimedes' principle [21]. The buoyancy force is an upward force exerted by a fluid that opposes the weight of the immersed object. Therefore, when the buoyancy force F_B, is greater than the vehicle weight, the vehicle starts to float and is carried away by the flow. This force can be expressed as:

$$F_B = \rho g V \tag{3}$$

where, ρ is the density of water, g is the acceleration due to gravity and V is the submerged volume of the vehicle [6].

The drag force can be defined as resistance to moving through a fluid [22]. In fluid dynamics, drag acts opposite to the relative motion of any object moving with respect to a surrounding fluid. The drag force relies on the area of changing momentum, fluid velocity and its density. The drag force F_D, can be expressed as:

$$F_D = \frac{1}{2}\rho C_D A_D v^2 \quad (4)$$

where, ρ is the density of water, C_D is the drag coefficient, A_D is the submerged area projected normal to the flow, and v is the flow velocity [18].

In a few studies, buoyancy force alone has caused floating instability of the vehicles and thus, the influence of lift force has been disregarded completely while estimating the vertical pushing force [6], [18] and [19]. However, when it comes to the hydrodynamic conditions (*i.e.* flow velocity), the vertical pushing force, which is composed of both buoyancy force and lift force, should be considered responsible for the floating instability [23]. Therefore, floating instability occurs when the buoyancy and lift forces exceed the weight of the car [24]. Thus, the vertical pushing force F_V, can be expressed as:

$$F_V = F_B + F_L \quad (5)$$

where, F_B is the buoyancy force and F_L is the lift force.

The lift force is a component of a force which is flowing past the surface of a body and acts perpendicular to the incoming flow direction. It contrasts with the drag force, which is the component of the surface force parallel to the flow direction [25]. It is a mechanical force generated by the interaction of a solid body with a fluid [26] which can be given as:

$$F_L = \frac{1}{2}\rho C_L A_L v^2 \quad (6)$$

where, ρ is the water density, C_L is the lift coefficient, A_L is the acting area by the lift force which is given by $A_L = (l_c \times b_c)$, where l_c and b_c are the length and width of the vehicle, respectively, and v is the flow velocity [27].

2.2 Typical Modes of Vehicle Instability

The loss of vehicle stability in floodwaters not only relies on the factors like water depth and flow velocity, but also on the physical and geometric properties of the immersed object. The mode of vehicle instability is influenced by several parameters which involves (i) position of the vehicle (parallel or perpendicular or side way to the flow), (ii) degree of submergence (partially or fully submerged), (iii) net weight and (iv) aerodynamic shape of the vehicle [16].

Vehicle orientation has been recognized as one of the potential critical conditions to first trigger vehicle instability. The position of the vehicle is an influential parameter as the drag force is concerned to the projected area normal to the flow. Therefore, it follows that the larger the affected area, the greater the drag force [18].

Similarly, a vehicle behaves in a different manner depending on the level of submergence, for instance, if the vehicle is partially submerged, then the threshold velocity increases for a decrease in the depth of flow, but if the vehicle is fully submerged, then the phenomenon is completely reversed [19].

Moreover, vehicle weight is another important parameter when it comes to stability in floodwater. The weight distribution of modern vehicles is not analogous as most of the vehicle weight is concentrated at the frontal lower part [24]. A vehicle with higher weight increases its chances of stability as greater water volume would be needed for the vehicle to become buoyant. Similarly, vehicles with higher ground clearance have more stability since deeper water is required to reach the vehicle chassis [23].

Lastly, vehicle aerodynamics cause drag mainly due to the shear stress. In the early 1930s, cars were designed in a series of boxes, that is, a box for passengers and driver, and a box for the engine, with everything else added on - fenders, headlights, spare tire, sunscreen, and so forth. Ten years later, the fenders were blended with the body which increased the frontal area. By early 1950s, the front end grown more rounded as fender and chassis blending had gone still further. However, by early 1960s the blending of chassis, headlights, fenders and other add-ons was complete. These timely changes somehow reduced the drag coefficient [28]. Bonham and Hattersley (1967) and Gordon and Stone (1973) used similar chassis design while performing the empirical investigations to determine the instability thresholds. However, compared to modern vehicles been used from 2010 onwards, those ancient cars were less aerodynamic. The modern vehicles are designed following the stream line body shape which lowers the friction drag, reduces the shear stress, and thus, lessens the drag coefficient. This dramatically reduces the pressure drag which makes it completely different from past vehicles [29]. However, modern cars are much lighter than older models and could easily become buoyant [30].

The hydrodynamic mechanisms by which the vehicle stability is lost can be recognized either by floating, sliding and toppling instability, as shown in Figure 3. The most frequent are the first two and, in most cases, instability occurs as a combination of both, floating and sliding. One of the reasons why modern cars are so easily swept away by even the shallowest of water depths is partially attributed to the sealing capacity. These cars are well sealed for minimizing the exposure to outside contaminants, such as carbon monoxide, noise, rain and wind. A better sealed space helps maintain better temperature control (air conditioning) within the vehicle itself. Under flooding conditions, better sealing does not allow water to seep inside the car, and thus, it provides a larger submerged volume to the buoyancy force to take effect. Therefore, even at lower depths, a lighter passenger vehicle could immediately compromise stability and float away when the base of the vehicle comes in contact with floodwater [31].

When the fluid is in a stationary state or the flow state is sub-critical, floating instability occurs when the buoyancy force exerted by water exceeds the gravitational force (vehicle weight), which can be given as $F_B > F_g$. This type of instability usually occurs when the flow depth is high. In case of flowing water (*i.e.* high flow velocities), the influence of lift force cannot be disregarded and, therefore, the mode of floating instability occurs when $F_V > F_g$.

For stationary vehicles (brakes applied), incipient motion for sliding occurs when drag force exerted by the incoming flow exceeds the frictional force, which is the product of the friction coefficient μ and immersed weight of the car [32]. Thus, the mode of sliding instability on a flat surface occurs when $F_D > F_R$.

A further mode of instability, which occurs due to overturning, is called toppling instability. However, this stability appears to be restricted to vehicles which are already sliding or floating [15]. Therefore, it has been excluded from further analysis.

3.0 EARLIER STUDIES (1967 - 1993)

The existing design guidelines and recommendations proposed for the limits of vehicle stability are based on the product of flow depth (D) and velocity (v) derived during the experimental investigations in the late 1960s and early 1970s (Bonham and Hattersley, 1967; Gordon and Stone, 1973) and theoretical analysis in the early 1990s (Keller and Mitsche, 1993). These guidelines are still being practiced as there was no significant research published in the intervening period between Keller and Mitsche's work (1993) and Teo *et al.*'s work (2010). However, today's vehicle on roads have undergone several gradual improvements over time, specifically in terms of shape and weight. These updated hydrodynamic designs and the use of lightweight metal chassis, however, cause greater buoyancy. Thus, results of earlier studies may no longer be applicable to contemporary vehicles and cannot be adopted permanently [15].

3.1 Bonham and Hattersley (1967)

The purpose of the study was to enable highway authorities to design safe causeways, with defined limits and warning indicator notices. Laboratory runs on the stability of a model Ford Falcon with a geometric length scale of 1:25 were conducted, as shown in Figure 4. The model vehicle was placed perpendicular to the flow direction and was restrained by fine threads, both vertically and horizontally. The threads passed over the pulleys out of the flume to floats contained in burettes. The loadings were then obtained by measuring the forces on those threads. The tests consisted of placing the car in a steady uniform discharge in the flume over a wide range of depths and flow velocities [33]. The vertical and lateral reactions recorded by the burette floats were then scaled up for a full-size Falcon. Once both the forces were obtained, the coefficient of friction μ, which would lead to loss of frictional stability, was described and is given by:

$$\mu = \frac{F_H}{F_v} \tag{7}$$

where, the horizontal reaction force F_H consists of momentum force and the pressure acting on the side of the car. The vertical reaction force F_v consists of buoyancy, vehicle weight and any vertical components of the momentum force acting on the curved shape of the car [15].

Specifying an appropriate frictional coefficient is required to define limiting flow values for vehicle stability. Lines of constant friction were produced for μ = 0.3 to 0.5 as shown in Figure 5. Finally, a coefficient friction of μ = 0.3 was adopted for most surfaces after corresponding with the various road experts and performing laboratory testing [34].

3.2 Gordon and Stone (1973)

Gordon and Stone (1973) conducted laboratory testing on the stability of the model Morris Mini sedan with a geometric length scale of 1:16 in a 1 m wide flume as shown in Figure 6 [35]. This vehicle was selected as it was considered most susceptible to losing stability in floodwaters among the range of the motor cars available at that time. The vehicle (exposed parallel to the flow direction) was restrained by fine threads, both vertically and horizontally, to measure the total horizontal and vertical reaction forces on the front and rear wheels. Three modes of resistance to the movement were considered. These included the vehicle parked in first gear (front wheels locked), the vehicle parked with handbrake on (rear wheels locked) and all wheels locked. The mode of all wheels locked was assumed non-conservative and the testing was undertaken only on the front wheels locked and the rear wheels locked condition. Once both the forces were obtained, the coefficients of friction representing the limit of stability were defined by the given equation:

$$\frac{\mathrm{F_H}}{\mu \mathrm{F}_v} = 1 \tag{8}$$

where, $\mathrm{F_H}$ is the measured horizontal reaction, (μ) is the coefficient of friction and F_v is the measured vertical reaction.

Figure 7(a) shows the raw test results of Gordon and Stone (1973) with the observed horizontal forces and front wheels' vertical reaction forces, whereas Figure 7(b) shows the results with the observed horizontal forces and rear wheels' vertical reaction forces [36].

To initiate vehicle movement as a function of velocity and depth, the lines of constant friction were derived for the vehicle parked in first gear (front wheels locked) and for the vehicle parked with handbrake on (rear wheels locked). The range of coefficients obtained from this study were between $\mu = 0.3$ (skidding on wet surfaces) and $\mu = 1.0$ (stationary on wet surface) [37]. Moreover, the friction coefficients measured for a stationary flooded tire in Canberra by UNSW (the University of New South Wales) ranged between 0.85 to 1.15, whereas the skidding road-tire coefficients of friction ranged between 0.16 to 0.48 (Woods *et al.*, 1960). These results indicate that the stationary value of $\mu = 0.3$ proposed by Bonham and Hattersley is likely conservative [15].

3.3 Keller and Mitsch (1993)

Keller and Mitsch (1993) undertook a purely theoretical study on the stability of both people and cars in flooding conditions. They provided a simple method for assessing the forces applied on a vehicle standing stationary in floodwater. Manufacturer specifications were obtained for the tested vehicles, including Toyota Corolla, Suzuki Swift, Ford Laser, Honda Civic, and Ford LTD. A vehicle slides when the horizontal force ($\mathrm{F_H}$) is equal to the vertical restoring force (F_v) which is a function of the assumed coefficient of friction and the vertical reaction force [3] and [38]. The mode of sliding instability was evaluated by considering the vehicle perpendicular to the flow direction, thus balancing the drag force induced by flow velocity and the frictional force at each car axle, taking into account the buoyancy and the vehicle weight. However, the corresponding criterion of stability threshold can be expressed as:

$$\mathrm{F_D} = \mathrm{F_R} \tag{9}$$

$$\frac{1}{2}\rho C_D A_D v^2 = \mu F_G \quad (10)$$

$$v = 2 \times \left(\frac{\mu F_G}{\rho C_D A_D}\right)^{\frac{1}{2}} \quad (11)$$

where, v is the incipient velocity, μ is the coefficient of friction which was set to 0.3 following Bonham and Hattersley (1967), F_G is the axle load in wet conditions (also the axle load in dry conditions minus the buoyancy force, which is distributed on the front and rear axles according to the location of the centre of buoyancy), ρ is the density of water, C_D is the drag coefficient which was set to 1.1 on the wheels, and 1.15 on the vehicle body with no sensitivity assessment evident, and A_D is the submerged area projected normal to the flow [39]. Figure 8(a) shows the theoretical results assessed for a range of vehicles as a function of depth and velocity, whereas Figure 8(b) shows the limiting D × v values which were found inconstant and non-linearly dependent on flow depth with the largest flow values tolerable at 0.15 to 0.25 m depth. The study concluded that a floating threshold between 0.34 and 0.40 m was required for the different model cars to float. However, the outcomes attained were not verified against any field or experimental data [15].

3.4 Summary

Table 1. shows the summary of the experimental and theoretical approaches by highlighting the important parameters and key findings of earlier studies.

3.5 Gaps and Challenges

The reported incidents about cars floating away from causeways in New South Wales in February 1967, led to studies on vehicle instability in floodwaters. Bonham and Hattersley (1967) initiated the experimental studies on this issue to determine the drag and lift effects of floodwaters on a vehicle placed in a flooded crossing. A similar experimental approach with different model vehicles was conducted later by Gordan and Stone (1973). Outcomes from both studies developed the limits of friction coefficients between the road surface and tires. Later, a theoretical approach to determine the incipient velocity for a flooded vehicle was proposed by Keller and Mitsche (1993), following the mechanical condition of sliding equilibrium. These studies involved medium-sized conventional cars. The vehicles chosen had different characteristics in terms of design, shape, ground clearance and weight, commonly found in large numbers on road sides. All experimental investigations followed the laws of similitude. Only limited orientations were selected, namely perpendicular and parallel to the approaching flows. Further, the behaviour of fully submerged vehicles was not covered.

The line of constant friction presented by Bonham and Hattersley (1967) ranged between μ =0.3 to μ=0.5, whereas the proposed final friction coefficient of μ=0.3 was adopted, which was confirmed as almost certainly adequate for most surfaces. However, the suggested final friction of coefficient proposed by Bonham and Hattersley (1967) was contradicted by Gordon and Stone (1973) as the range of coefficients obtained from his study were between μ=0.3 (skidding on wet surfaces) and μ=1.0 (stationary on wet surface). Further, the values of friction coefficients measured by Yandell (1973) and Woods *et al.* (1960) ranged between 0.85 and 1.15 and between 0.16 to 0.48, for the stationary coefficients and the skidding values, respectively [40] and [41]. Therefore, these results indicate that the stationary value of μ

=0.3 assumed by Bonham and Hattersley (1967) is likely conservative. However, the theoretical approach carried by Keller and Mitsch (1993) adopted the friction coefficient of μ=0.3, suggested by Bonham and Hattersley (1967). Moreover, the drag coefficients of 1.15 on the vehicle body and 1.1 on the wheels were adopted with no apparent sensitivity assessment. The outcomes attained through this theoretical assessment were not verified against any field or experimental data.

4.0 RECENT STUDIES (2010 – 2017)

No significant research published in the field of vehicle stability after the theoretical analyses proposed by Keller and Mitsch (1993) until 2010. Therefore, the existing safety guidelines on vehicle stability in flooded paths are based on the product of flow depth and velocity proposed in the earlier inquiries (1967-1993). Herein an attempt was made to further explore stability criteria for stationary vehicles (modern cars) proposed by several authors in recent years. This involves the work of Teo *et al*. (2010), Xia *et al*. (2010), Shu *et al*. (2011), Toda *et al*. (2013), Xia *et al*. (2013) and Martínez-Gomariz *et al*. (2017). Car designs and roadway conditions had improved with time; thus, a variety of dimensions were reported. Some of the hydrodynamic behaviours reported might have improved the stability, but probably in contrast, vehicles with smaller ground clearance have lower stability when flooded [3].

4.1 Teo *et al*. (2010)

Teo *et al*. (2010) investigated the hydraulic behaviours of vehicles in urban floodplains through laboratory experiments in two hydraulic flumes having different widths, namely small (0.3 m) and wide (1.2 m), as shown in Figure 9. A Mini Cooper, BMW M5, and Mitsubishi Pajero with scales of 1:43 (small scale) and 1:18 (large scale) were adopted. These vehicles were chosen because they were relatively light (in weight) and commonly found on road sides and parking lots. Experimental tests were carried out on a flat rough bed surface. To simulate the handbrake being left on, all tires were glued to restrict free rotation. Furthermore, the vehicles were made water tight with plastic tapes attached and glued around the edges. The experimental results obtained from the small-scale model (1:43) in the smaller flume were then scaled up (1:18) using the laws of hydraulic similarity. The results' accuracy were validated with the experimental results obtained for the same scale in the wider flume. The trends of the predicted values were in general agreement with the trends observed through the experimental approach [18].

The study outcomes indicated that, under partial submergence, the threshold velocities needed for the initial movement of the car decrease with the increasing water depth for all the vehicles, as shown in Figure 10 (rear ends facing the flow). This trend remained continuous for all the vehicles until they were fully submerged. The vehicle's frictional force and fluid velocity were the more influencing factors to cause sliding instability as the projected area as well as the aerodynamics had little to do with the movement. Conversely, under full submergence, the condition was completely reversed because of high-water depths (above the height of vehicle chassis), which means that the drag force imposed by the incoming flows on the vehicle's projected area was more dominant.

The critical conditions for vehicle instability thresholds were established by varying the vehicle orientations, as shown in Figure 11. Two parameters, namely water depth and flow velocity, were within high threshold values, especially when the vehicles' actual front and rear ends were facing the flow. This was due to the smoothing rear and front ends, which reduced the hydraulic drag due to the vehicles' aerodynamic design. On the other hand, when the vehicles were positioned perpendicular to the flow direction, smaller threshold values were required to initiate instability. This was due to the availability of the larger bluff area projected normal to the flow, which reduced the cross-sectional area of the flow through the vehicles and, subsequently, the drag forces and the blockage effects were increased [30].

It has been further suggested that, under partially or fully submerged conditions, the drag force induced by the incoming flow is just balanced by the frictional force preventing the vehicle from sliding. Thus, the corresponding criterion of instability threshold is given by:

$$F_D = F_R \tag{12}$$

$$\frac{1}{2}\rho C_D A_D\, v^2 = \mu F_G \tag{13}$$

$$v = \left[\frac{2\mu F_G}{\rho C_D A_D}\right]^{\frac{1}{2}} \tag{14}$$

where, v is the velocity at the threshold of instability, μ is the friction coefficient, F_G is the axle load in wet conditions (also the axle load in dry conditions minus the buoyancy force on the vehicle, which is distributed on the front and rear axles according to the location of the centre of buoyancy), ρ is the density of water, C_D is the drag coefficient set at 1.1 if the water level is below the vehicle chassis and 1.15 if it is above the vehicle chassis and A_D is the submerged area projected normal to the flow [19].

4.2 Xia *et al.* (2010)

Xia *et al.* (2010) derived a formula to predict the incipient velocity of flooded vehicles under fully submerged condition based on the mechanical condition of sliding equilibrium. The formula was validated based on the outcomes obtained from experimental study of Teo *et al.* (2010). Three tested small-scale (1:43) model vehicles (a Mini Cooper, a BMW M5, and a Mitsubishi Pajero) were considered to determine the two parameters in the derived formula. The experimental data obtained for larger-scale (1:18) model vehicles was used to validate the prediction accuracy of this formula. In the analysis of vehicle stability to determine the expression for each force and the potential mode of incipient motion, few assumptions were included: (1) due to geometric similarity for the model and prototype, the similarity law of the drag coefficient was fulfilled, (2) the vehicle wheels were all locked and only the motion pattern of vehicle sliding was considered, (3) the flume bed was made of rough bakelite and the tire of the model were made from the same rubber material as of the prototype thus, ensuring that the similarity law of the friction coefficient was also met and (4) only one incoming flow direction (rear end of the vehicle facing the flow) was considered [27]. The formula of incipient velocity for flooded vehicles proposed by Xia *et al.* (2010) has been simplified in the steps below.

The frictional force (F_R) to resist the vehicle from sliding can be given as:

$$F_R = \mu F_G \tag{15}$$

$$F_G = F_g - F_B - F_L \tag{16}$$

where, F_G is the submerged weight of the vehicle, F_g is total weight of the vehicle, F_B is the buoyancy force and F_L is the lift force. Thus, Eq. (15) can be re-written as:

$$F_R = \mu\left[(\gamma_c - \gamma_f).V_c - C_L A_L \gamma_f \frac{{u_b}^2}{2g}\right] \tag{17}$$

Since the study was conducted considering only the mode of sliding instability, the corresponding criterion of instability threshold can be given as:

$$F_D = F_R \tag{18}$$

$$C_D A_D \gamma_f \frac{{u_b}^2}{2g} = \mu\left[(\gamma_c - \gamma_f).V_c - C_L A_L \gamma_f \frac{{u_b}^2}{2g}\right] \tag{19}$$

$$u_b = \sqrt{2g\left(\frac{\rho_c - \rho_f}{\rho_f}\right)}\sqrt{\frac{\mu V_c}{C_D A_D + \mu C_L A_L}} \tag{20}$$

Substituting the values of V_c (vehicle volume), A_D (submerged area affected by drag force) and A_L (submerged area affected by the lift force) in Eq. (20) gives:

$$u_b = \sqrt{2g\left(\frac{\rho_c - \rho_f}{\rho_f}\right)}\sqrt{\mu\frac{a_v l_c b_c h_c}{C_D a_d h_c b_c + \mu C_L a_l l_c b_c}} \tag{21}$$

However, it was assumed that $l_c = a_h h_c$, where h_c is the vehicle height but the description of a_h has not been defined therefore, putting the value of l_c in Eq. (21) gives:

$$u_b = \sqrt{2g\left(\frac{\rho_c - \rho_f}{\rho_f}\right)}\sqrt{h_c}\sqrt{\mu\left(\frac{a_v}{\left(C_D\frac{a_d}{a_h} + \mu C_L a_l\right)}\right)} \tag{22}$$

Let $\alpha_1 = \sqrt{\mu\left(\frac{a_v}{\left(C_D\frac{a_d}{a_h} + \mu C_L a_l\right)}\right)}$, then Eq. (22) can be re-written as:

$$u_b = \sqrt{2g\left(\frac{\rho_c - \rho_f}{\rho_f}\right)h_c} \times \alpha_1 \tag{23}$$

The near-bed velocity u_b cannot be calculated easily and, therefore, the depth-averaged velocity U following the vertical velocity distribution is introduced. It can be calculated as $u = (1 + \beta)\left({}^{y}/_{h}\right)^{\beta} U$, where β is an empirical coefficient, y is the vertical distance from the bed and u is the velocity at y. If the representative height of u_b is $\alpha_b h_c$ where α_b is coefficient related to the vehicle height, then:

$$u_b = (1 + \beta)\left({}^{\alpha_b h_c}/_{h}\right)^{\beta} U \tag{24}$$

Substituting the value of u_b from Eq. (23) in Eq. (24), then the incipient velocity U_c, for the vehicles in floodwaters can be given as:

$$U_c = \frac{\sqrt{2g\left(\frac{\rho_c - \rho_f}{\rho_f}\right)h_c} \times \alpha_1}{(1+\beta)\left(\frac{\alpha_b h_c}{h}\right)^{\beta}} \tag{25}$$

Let $\alpha = {}^{\alpha_1}\!/_{[(1+m)a_b{}^{\beta}]}$, then U_c can be re-written as:

$$U_c = \alpha \times \left(\frac{h}{h_c}\right)^{\beta} \sqrt{2g\left(\frac{\rho_c - \rho_f}{\rho_f}\right)h_c} \tag{26}$$

where U_c is the incipient velocity for the flooded vehicles, α and β are the empirical parameters for each vehicle, h is the water depth, h_c is the vehicle height, ρ_c is the vehicle density and ρ_f is water density.

4.3 Shu *et al.* (2011)

Shu *et al.* (2011) investigated the stability criteria for partially submerged vehicles by deriving the mechanics-based formula of incipient velocity. The flume experiments were conducted on wet carpet at a scale of 1:18 using three types of die-cast vehicles (Ford Focus, Ford Transit, Volvo XC90) by strictly following the similarity principles of shape, motion, and forces. The density of the selected model vehicles was nearly equal to that of the corresponding prototype. The incipient motion of the vehicles was noted when of all the tires were locked and positioned at two different orientation angles, namely 0° and 180°. The orientation angle of 0° meant that the vehicle front was facing the direction of approaching flow, as shown in Figure 12, while the orientation angle of 180° meant that the vehicle rear was facing the direction of the incoming flow. The friction coefficient μ between the wet carpet and the tire for various models was estimated in the flume. The vehicle was placed on the wet carpet and then being manually pulled by a spring balance. As the vehicle started to move, the value of the force, as shown on the balance, was recorded.

It has been stated that the effective weight F_G for a partially-submerged vehicle can be given as:

$$F_G = F_g - F_B \tag{27}$$

As the vehicle starts *float* under a specified depth, the effective weight F_G will become zero. Therefore Eq. (27) can be re-written as:

$$F_g = F_B \tag{28}$$

where, F_g is total weight of the vehicle which can be given as:

$$F_g = \gamma_c V_c = a_c l_c b_c h_c \gamma_c \tag{29}$$

where, a_c is a coefficient representing the proportion of effective volume, l_c is the vehicle length, b_c is the vehicle width, h_c is the vehicle height and γ_c is the specific weight of the car.

Similarly, F_B is the buoyancy force which can be given as:

$$F_b = \gamma_f V_f = a_f l_c b_c h_f \gamma_f \tag{30}$$

Substituting the values of F_g and F_B in Eq. (27) gives:

$$F_G = a_c l_c b_c (h_c \gamma_c - h_f \gamma_f R_f) \tag{31}$$

The frictional force, F_R to resist the vehicle from sliding can be given as:

$$F_R = \mu F_G \tag{32}$$

Substituting the value of F_G from Eq. (31) into Eq. (32) gives:

$$F_R = \mu[a_c l_c b_c (h_c \gamma_c - h_f \gamma_f R_f)] \tag{33}$$

As already defined in the previous section, the corresponding criterion of sliding instability can be given as:

$$F_D = F_R \tag{34}$$

Substituting the values of F_D and F_R into Eq. (34) gives:

$$u_b = \sqrt{\frac{\mu a_c}{a_d C_d}} \sqrt{2 g l_c \left(\frac{h_c \rho_c}{h_f \rho_f} - R_f\right)} \tag{35}$$

The near-bed velocity u_b cannot be calculated easily and, therefore, the depth-averaged velocity U following the vertical velocity distribution is introduced. It can be calculated as $u = (1+\beta)U/\left({}^{y}/_{h}\right)^{\beta}$, where β is an empirical coefficient, y is the vertical distance from the bed, and u is the velocity at y. Assuming that the representative height of u_b is $\alpha_b h_c$, in which α_b is a coefficient related to the vehicle height, then:

$$u_b = (1+\beta)U/\left({}^{\alpha_b h_c}/_{h}\right)^{\beta} \tag{36}$$

Substituting the value of u_b from Eq. (35) into Eq. (36), then the incipient velocity U_c, for the partially submerged vehicle in floodwaters can be given as:

$$U_c = \frac{1}{(1+\beta){\alpha_b}^{\beta}} \sqrt{\frac{\mu a_c}{a_d C_d}} \left(\frac{h_f}{h_c}\right)^{\beta} \sqrt{2 g l_c \left(\frac{h_c \rho_c}{h_f \rho_f} - R_f\right)} \tag{37}$$

Let $\alpha = \frac{1}{(1+\beta){\alpha_b}^{\beta}} \sqrt{\frac{\mu a_c}{a_d C_d}}$, then Eq. (37) can be re-written as:

$$U_c = \alpha \left(\frac{h_f}{h_c}\right)^{\beta} \sqrt{2 g l_c \left(\frac{h_c \rho_c}{h_f \rho_f} - R_f\right)} \tag{38}$$

where, U_c is the incipient velocity for partially submerged vehicles in floodwaters, $\propto$ and β are the empirical parameters for each vehicle, h_f is the water depth, h_c is the vehicle height, l_c is the car length, ρ_c is the vehicle density, ρ_f is the density of water and R_f is the ratio of vehicle height, and density to the buoyancy depth and water density.

The predicted velocities using the formula agreed well with the corresponding measured values with the correlation coefficient $R^2 = 0.97$, ensuring that if the incoming flow depth is less than the vehicle height (partially submerged), then the threshold velocity increased with a decrease in the depth of flow as shown in Figure 13 [6].

4.4 Toda *et al.* (2013)

Toda *et al.* (2013) conducted experimental studies on critical incipient floating conditions of the vehicles in floodwaters in a 1.0 m wide mortar flume. The study was performed at Ujigawa Open Laboratory, Disaster Prevention Research Institute, Kyoto University, as shown in Figure 14. Two types of model vehicles were selected; a sedan-type and a minivan-type with 1:10 and 1:18 scales, respectively. Following the strict similarity principles, it was ensured that the model density was equal to the prototype. The model vehicle weight was adjusted by small steel plates until the same density as the corresponding prototype was obtained. Further, while analysing the forces on the flooded vehicles, the lift force has also been considered. As the water depth starts to increase around the vicinity of the vehicles, the lift force, together with the buoyancy force, reduces the gravitational force. The decreased buoyancy was considered by allowing the water inside the partially submerged vehicle. The friction coefficients were measured using a spring balance for the vehicle positioned at 0° and 90°. At 0°, the hand brake condition was kept on, whereas at 90°, the wheels could rotate freely for both model vehicles. The friction coefficients obtained for the sedan-type ranged between 0.26 (0°) and 0.57 (90°), whereas for the minivan-type it was found to be 0.42 (0°) and 0.65 (90°), respectively [42]. The study proposed the resultant equation of stability based on the mode of sliding instability which can be described as:

$$F_D = F_R \tag{39}$$

where, F_D is the drag force acting on a side of vehicle and F_R is the frictional force. Moreover, the lift force and buoyancy force are mainly formed by the vertical pushing force when it comes to hydrodynamic conditions [23]. Thus, the vertical pushing force F_V can be given as:

$$F_V = F_B + F_L \tag{40}$$

where, F_B is the buoyancy force and F_L is the lift force. Hence, the general formula for the friction force can be expressed as:

$$F_R = \mu F_G \tag{41}$$

$$F_R = \mu(M_c g - F_B - F_L) \tag{42}$$

where, M_c is the mass of the car, g is the gravitational force, F_B is the buoyancy force and F_L is the lift force. Substituting Eq. (42) into Eq. (39) gives:

$$\frac{F_D}{\mu(M_c g - F_B - F_L)} = 1 \tag{43}$$

The drag coefficient (C_D) of partially submerged cars in the flooding flow was obtained with the above equation, which was then used to determine the relation between drag coefficient and relative water depth. Moreover, the critical incipient floating conditions were obtained from the experimental results, which were later proposed for real cars. The study concluded that, if the water depth is more than 0.5 m and the flow velocity is higher than 2.0 m/s, then the floating instability of the sedan-type vehicles (prototype) is likely to occur.

4.5 Xia *et al.* (2013)

A variation of the Shu *et al.* (2011) formula was proposed by Xia *et al.* (2013). The experimental runs were conducted in a flume of the Experimental Hall for Sediment and Flood Control Engineering, Wuhan University, China. The horizontal flume was 1.2 m wide, 60 m long and with the bed covered by a thin cement layer and two glass sides. To obtain the conditions of water depth and corresponding velocity at the threshold of vehicle instability, three orientation angles (0°, 180° and 90°), as shown Figure 15, and two ground slopes (1:50 and 1:100) were selected. Two sets of different die-cast model vehicles were selected (Honda Accord and Audi Q7) at the scale ratio of 1:14 (larger die-cast-model) and 1:24 (small die-cast-model) strictly following the laws of similarity. The wheels of the vehicle were locked; thus, only the incipient motion under sliding was considered. The physical models were meant to evaluate how the vehicle's size, kerb weight and design shape could affect the threshold of vehicle instability in floodwaters. In free-surface flows, the effects of gravity are predominant and the model-prototype similarity was generally satisfied following the scaling criterion of Froude similarity. According to the requirements for kinematic similarity, the scale ratio of the inertia force to the gravity force gives the relationship between the scale ratios of velocity and length, thus satisfying the Froude similarity. Dynamic similarity implies that the ratios of the prototype forces to model forces are equal if the density of a model vehicle is equal to the value of a prototype vehicle [43].

To determine the threshold of vehicle instability, the corresponding depth-averaged velocity and the incoming depth were recorded when the submerged vehicle started to slide by adjusting the discharge in the flume gradually. The friction coefficients were measured in the flume for the two model vehicles and the mean coefficient friction was 0.75 for the case where the inflow direction was perpendicular to the vehicle length and 0.25 where the inflow direction was parallel to the vehicle length. The range of friction coefficients measured for the model vehicles corresponded well with the prototype range [44].

The test results indicated that there was not a substantial difference in the condition of incipient motion for the orientation angles of 0° and 180° because the submerged area, projected normal to the incoming flows for the former, was almost equivalent to that for the latter for a partially submerged vehicle. However, at 90°, the incipient velocity required to make the vehicles unstable was low for both car models, as shown in Figure 16. The study further suggested that, compared to the flat ground, the incipient velocity required to make a car unstable at different slopes was reduced somehow. When the ground slope is at an angle θ, the driving force causing the vehicle to slip increases, and the value of normal force is reduced.

The governing equation to determine the incipient velocity proposed by Shu *et al.* (2011) was applicable to the vehicles positioned parallel to the flow direction. However, Xia *et al.* (2013) modified the same equation for the vehicles positioned perpendicular to the flow direction. Therefore, the proposed resultant equation of stability based on the mode of sliding stability can be given as:

$$F_D = F_R \tag{44}$$

where, F_D is the drag force acting on a side of vehicle which can be given in the general form as:

$$F_D = C_D A_D \gamma_f \frac{{u_b}^2}{2g} \tag{45}$$

where, C_D is the drag coefficient, A_D is the submerged area projected normal to the flow, $A_D = a_d(h_c l_c)$, in which a_d is an empirical coefficient and $(h_c l_c)$ is the submerged area (*side of the vehicle*), u_b is the near-bed velocity and g is the acceleration due to gravity. Substituting Eqs. (33) and (45) into Eq. (44) gives:

$$C_D A_D \gamma_f \frac{{u_b}^2}{2g} = \mu[a_c l_c b_c(h_c\gamma_c - h_f\gamma_f R_f)] \tag{46}$$

$$u_b = \sqrt{\frac{\mu a_c}{a_d C_d}}\sqrt{2_g b_c\left(\frac{h_c\rho_c}{h_f\rho_f} - R_f\right)} \tag{47}$$

The near-bed velocity u_b cannot be calculated easily and therefore the depth-averaged velocity U following the vertical velocity distribution is introduced. It can be calculated as $u = (1+\beta)U/\left({}^{y}/_{h}\right)^{\beta}$, where β is an empirical coefficient, y is the vertical distance from the bed and u is the velocity at y. If the representative height of u_b is $\alpha_b h_c$, in which α_b is coefficient related to the vehicle height, then:

$$u_b = (1+\beta)U/\left({}^{\alpha_b h_c}/_{h}\right)^{\beta} \tag{48}$$

Substituting u_b from Eq. (47) in Eq. (48), then the incipient velocity U_c, for the partially submerged vehicle in floodwaters can be given as:

$$U_c = \frac{1}{(1+\beta){\alpha_b}^{\beta}}\sqrt{\frac{\mu a_c}{a_d C_d}}\left(\frac{h_f}{h_c}\right)^{\beta}\sqrt{2_g b_c\left(\frac{h_c\rho_c}{h_f\rho_f} - R_f\right)} \tag{49}$$

Let $\alpha = \frac{1}{(1+\beta){\alpha_b}^{\beta}}\sqrt{\frac{\mu a_c}{a_d C_d}}$, then Eq. (49) can be re-written as:

$$U_c = \alpha\left(\frac{h_f}{h_c}\right)^{\beta}\sqrt{2_g b_c\left(\frac{h_c\rho_c}{h_f\rho_f} - R_f\right)} \tag{50}$$

where, U_c is the incipient velocity for partially submerged vehicles in floodwaters, ∝ and β are the empirical parameters for each vehicle, h_f is the water depth, h_c is the vehicle height, b_c is the vehicle width, ρ_c is the vehicle density, ρ_f is the density of water and R_f is the ratio of vehicle height, and density to the buoyancy depth and water density.

4.6 Martínez-Gomariz *et al.* (2017)

Martínez-Gomariz *et al.* (2017) proposed a new methodology to obtain the stability threshold for any real vehicles exposed to flooding involving the analysis of both friction and buoyancy effects. The experimental tests were carried out in the flume of hydraulic laboratory of the Technical University of Catalonia (Spain), as shown in Figure 17. The horizontal flume was 20 m long and has a square cross section 60 × 60 cm. The flume was made of glass walls and a Bakelite bed, with slopes ranging from 0 to 4%. The flume was capable of obtaining multiple combinations of discharges and slopes, hence varying water depths and velocities. In addition, it was possible to test the scale model vehicles in a flat zone.

A range of twelve model cars with three different model scales (1:14, 1:18 and 1:24) were selected to conduct experiments following the initial assumptions of Froude similarity. It was ensured that the density of the model vehicle was the same as the corresponding prototype. Moreover, to prevent water leakage, each model vehicle was filled with light form so that the weight before and after the test remains the same and, thus, no variability in the buoyancy conditions can be obtained [23].

4.6.1 Friction coefficient and buoyancy tests

The friction coefficient depends on the ground surface, tire material and on the conditions of both the tires and the road. A comprehensive study was performed to determine the friction coefficient between the tires of the scaled model vehicles and the surface of the local slope set-up. The vehicle was positioned on the wetted flat surface and the force was applied manually through a spring balance, as shown in Figure 18. This frictional force, indicated by the spring balance, divided by the scaled model vehicle weight is the value of friction coefficient. The range of friction coefficients (μ) obtained for variety of scaled vehicles ranged between 0.52 to 0.62.

The purpose of conducting the buoyancy test was to reach the instability of the model vehicle without considering the flow velocity. A glass box of 38.9 × 18.9 cm² plan area was used, sufficient enough to accommodate the model as shown in Figure 19. The box was slowly filled with water through a small 2 cm diameter plastic pipe until no wheel was in contact with the ground. At this point, the buoyancy depth (h_b) was assumed to be attained, which was then scaled up to the corresponding prototype. The water volume displaced by the vehicle was calculated by the difference between the water depth in the recipient before and after the placement of the model vehicle. Thus, a theoretical verification was carried out by comparing the weight of the model vehicle with the weight of the displaced volume.

To define the stability threshold fully, theoretic buoyancy depth, h_b can be calculated by:

$$h_b = \frac{M_c}{\rho_w . l_c . b_c} + GC \tag{51}$$

where, h_b is the buoyancy depth, M_c is the weight of the vehicle, ρ_w is the water density, l_c is the length of the vehicle, b_c is the width of the vehicle and GC is the ground clearance of the vehicle. The derivation of this equation responds to the same criterion conducted to verify the results of experimental buoyancy tests, which was demonstrated to be accurate [23].

4.6.2 Methodology for obtaining stability thresholds

To classify every vehicle's stability level, three variables were considered, namely ground clearance, kerb weight and vehicle plan area. The first case states that, in order to reach the chassis of the vehicle with high ground clearance, higher water depth is needed; thus, buoyancy will start to take effect later. In the second case, a greater water volume displaced by the vehicle is needed to become buoyant for higher weights. On the other hand, greater vehicles' plan areas need lower water depths to reach the water volume displaced by the vehicle needed to become buoyant [23]. Based on that reasoning, a stability coefficient (SC) was derived:

$$\mathrm{SC} = \frac{\mathrm{GC.M_c}}{\mathrm{PA}} \tag{52}$$

where, GC is the ground clearance, M_c is the kerb weight and PA is the plan area. Since the friction coefficient (μ) between tire and ground enables the most general comparison between vehicle stability; therefore, the modified stability coefficient can be given as:

$$\mathrm{SC_{mod}} = \frac{\mathrm{GC.M_c}}{\mathrm{PA}}.\mu \tag{53}$$

The range of modified stability coefficient for the selected model ranged from 10.3 $kg.m^{-1}$ up to 50.3 $kg.m^{-1}$, whereas a velocity × depth function ($v \times y$) was used to represent the total set of instability points for all the scaled models. The scatterplot of modified stability coefficient and ($v \times y$) constant function showed an adequate linear correlation between both variable with a square correlation coefficient (R^2) of 0.93 and therefore the equation of straight line can be given as:

$$(v \times y) = 0.0158\,.\,\mathrm{SC_{mod}} + 0.32 \tag{54}$$

4.7 Summary

Table 2 shows the summary of the experimental and theoretical approaches conducted in the recent years, highlighting the important parameters and the research gaps by analyzing the key findings of the articles.

4.8 Gaps and Challenges

The authors prefer the friction coefficient proposed by Bonham and Hattersley (1967), whereas few authors believed that the friction coefficient could best be determined experimentally. The buoyancy depth, which can also be referred to as the critical water depth, has only been suggested by a few authors including Toda *et al.* (2013), Xia *et al.* (2013) and Martínez-Gomariz *et al.* (2017). Conversely, other works proposed different ranges of flow depths and velocities, defining the incipient motion of flooded vehicles. These values were simplistic as the design guidelines for vehicle stability were generally based on the product of flow depth (D) and velocity (v) derived during experimental investigations. The influence of lift force was first introduced by Xia *et al.* (2010) while proposing the formula of incipient velocity for flooded vehicles. Lift force is an important parameter which had not been considered by several studies before Xia *et al.* (2010). However, reliable assessment of lift coefficients for cars in floods is still not clearly understood and need further investigation. Teo *et al.* (2010) were the first to explore the divergent paths by investigating the hydraulic behaviours of modern vehicles in urban floodplains. Several modern vehicles of varying design characteristics were being investigated, including medium sized conventional cars and SUVs 'Sport-utility (vehicle)' with raised ground clearance. However, Martínez-Gomariz *et al.* (2017) conducted experimental studies with three different model scales (1:14, 1:18 and 1:24), including a wide range of modern vehicles commonly available on roads, which made this the most comprehensive research study to date.

Teo *et al.* (2010) and Xia *et al.* (2010) conducted their studies at the University of Cardiff on the same line of research. The study conducted by Teo *et al.* (2010) stated that the Froude similarity has been ensured, but the weight of the scaled models was not modified according to the Froude similarity [3]. To ensure Froude similarity, the model weight should be adapted based on the equal prototype and model densities, not only considering the scale ratio, which is just appropriate for lengths, not weights. Therefore, the experimental results obtained from the small-scale model (1:43) in the smaller flume scaled up to larger scale (1:18) were inadequate because the scale model densities (1:43 and 1:18) were not comparable. Therefore, the proposed thresholds for prototypes are considered unsafe since the velocities were consistent only for vehicles that were much heavier than the real ones.

Xia *et al.* (2010) proposed a formula to predict the incipient velocity of flooded vehicles according to the mechanical condition of sliding equilibrium. This formula was validated based on the experimental results of Teo *et al.* (2010) for the three-tested small-scale (1:43) vehicle models. Being aware that the weights of the scaled models were not adjusted accordingly to ensure Froude similarity, it was stated that: 'In the experiments, the density of the vehicles was significantly greater than in the prototype one. This meant that the model vehicles would be more submerged at the point of initiation of motion in the flume than in the prototype case'. To overcome such limitations, a relative density term was included in the derived formula. Nevertheless, the buoyancy depth was not taken into account in this study; thus, the representation of the derived formula reached depths even beyond vehicle heights. Further, the parameter of lift force was introduced in the derived formula. However, while conducting the experimental runs Teo *et al.* (2010) disregarded the parameter of lift force while estimating the influence of vertical pushing force.

A semi-empirical formula for critical motion conditions for partially submerged vehicles was derived by Shu *et al.* (2011), offering a new approach where the buoyancy depth was considered. The experimental runs, conducted by Shu *et al.* (2011), ensured Froude similarity as the adapted weight, density and scale ratio of the model was equal to the prototype. To derive the incipient velocity formula, the forces acting on the partially submerged vehicle in the first motion, *i.e.* sliding, were introduced. However, the influence of lift force was disregarded which was considered by Xia *et al.* (2010) for the estimation of incipient velocity formula. The study agreed further with Gordon and Stone (1973)'s work, confirming that a friction coefficient was unlikely to be obtained. Therefore, several measured values of friction coefficients were proposed. However, the authors believed that friction coefficients obtained from a wet carpet would not truly represent the actual Manning's roughness coefficients of a typical road surface.

Other experimental studies were conducted by Toda *et al.* (2013) at Ujigawa Open Laboratory, Disaster Prevention Research Institute, Kyoto University, Japan. A new approach was adopted in this case where the void space rate of a car and the additional mass inside a car, such as luggage and passengers, were also taken into account. These parameters were later adapted by Oshikawa *et al.* (2014) while studying the risk evaluation for a compact car (1:24) and a sport utility vehicle (1:24) in a flood situation [45]. The empirical investigation, performed by Toda *et al.* (2013), highlighted that the density of the model vehicle (sedan-type car, 1:10) was adjusted using the small steel plates until the same density as the corresponding prototype was obtained. The sedan-type car was 0.47 m long, 0.20 m wide, 0.15 m high with a weight of 1.350 kg which was originally 1.216 kg without steel plate. The volume of the steel plate used for the adjustment has not been mentioned; further, the maximum water depth attained for the sedan-type car was 0.069 m. Therefore, while determining the incipient motion condition, if those steel plates were attached to the vehicle chassis below the maximum water depth, then this additional volume could have affected the vehicle's submerged fractions to estimate buoyancy and lift forces.

Xia *et al.* (2013) modified the incipient velocity formula proposed by Shu *et al.* (2011) by considering the incoming flow direction relative to the vehicle length. While estimating the drag force for a vehicle positioned parallel to the flow, Shu *et al.* (2011) suggested that the influence of drag force would be either at the front or the rear of the vehicle; therefore, the affected drag area was given as $A_D = a_d(h_c b_c)$, in which a_d is an empirical coefficient, h_c is the height of the car and b_c is the vehicle width. Xia *et al.* (2013) suggested that, when the vehicle is positioned perpendicular to the flow direction, the influence of the drag force in that case would be at the side end of the vehicle. Therefore, the affected drag area in the new equation was given as $A_D = a_d(h_c l_c)$, in which a_d is an empirical coefficient, h_c is the height of the car and l_c is the vehicle length. Moreover, looking back at the formula proposed by Xia *et al.* (2010), the important parameter of lift force to predict the incipient velocity of flooded vehicles was considered. However, this parameter was disregarded by Xia *et al.* (2013) while modifying the equation proposed by Shu *et al.* (2011).

Martínez-Gomariz *et al.* (2017), undertook further experimental studies to explore a wider range of issues, such as the thresholds of vehicle instability, effects of vehicle orientations, ground gradient, and the consideration of the effects of buoyancy decrease from water inside the vehicle [46]. A modified stability coefficient (SC_{mod}) was proposed to classify the stability level of every vehicle. This coefficient was based on four variables, namely ground clearance, kerb weight, vehicle plan area and friction coefficient. Based on the adequate linear correlation obtained from the scatter plot of the variables ($v \times y$) constant function and modified stability coefficient, a new approach for obtaining the stability thresholds of any real car was proposed. Moreover, to fully define the stability threshold, a formula to determine the theoretic depth was introduced. Further, it was ensured that there was no variability in the buoyancy conditions, so the weight before and after the test remains the same. This was done by filling the interior of each scale model with light foam, unlike in the study of Toda *et al.* (2013). However, other studies have considered the interaction of vehicles with other infrastructure, such as bridges, revealing how blockages could significantly alter flood flow paths and depths [47].

Herein the detailed description of an incipient velocity formula for a non-stationary vehicle attempting to cross a flat flooded roadway has been proposed under the consideration of two new parameters, namely rolling friction and driving force for the very first time. The critical conditions obtained using the scaled model (Perodua Viva, 1:10) agreed well with the calculations from the derived formula. Since the current article is a review paper therefore, the experimental outcomes have not been shared and the focus has remained more on the description of proposed formulation.

5.0 FUTURE WORKS

Water is essentially a powerful component, strong enough to move vehicles at the lowest hydraulic parameters. The flow orientation, as well as the geometric and physical characteristics of the vehicle model, also affect the way floodwaters control the vehicle. *Hence, what are the hydraulic parameters and limiting threshold conditions in which a vehicle, successfully progresses until it encounters vehicle instability?* This research attempts to examine such conditions. The detailed formulation of an incipient velocity equation has been proposed. The formula has been validated through extensive experimental testing, carried out in a special set up, to closely imitate a vehicle moving perpendicular to the direction of flow on a flat roadway. The study was limited to a passenger car controlled to be partially submerged under the influence of sub-critical flows. Various hydrodynamic data on the response of the vehicle towards the incoming flows have been presented, which was later validated through the proposed formula.

5.1 Hydrodynamic Forces on a Moving Vehicle

The impact of hydrodynamic forces pertaining to static vehicles (parked) have been discussed in detail, in the former section. Due to applied braking conditions, the frictional force on the static vehicles mainly focus on the static friction coefficient. However, when it comes to the instability mechanism of a non-stationary vehicle, several parameters, including the type of friction between the tires and the ground surface, differ. For instance, when a vehicle attempts to cross a flooded street (perpendicular to the flow direction), then the impact of friction force acts in two directions, namely in the direction of incoming flow (F_R) and in the direction of tires rotation (F_{RO}). In the current investigation, the friction coefficients for both directions were experimentally determined. In addition to this, a supplementary force caused by the vehicle engine, also known as driving force (F_{DV}), has been introduced, which opposes the drag force caused by the incoming flow. Concerning drag force, its impact on a non-static vehicle differs. For non-static cars, the drag does not only affect the side end of the vehicle facing the flow direction but also the frontal vehicle chassis intersecting with floodwater. Herein the proposed formulation is limited to sub-critical flow states. While performing the experimental runs, the impact of drag force at the frontal end of the vehicle was found insignificant due to low flow velocities; therefore, its impact in that direction has been disregarded in this study from further consideration. However, its impact may vary for other flow states, *i.e.,* critical and super-critical. Lastly, the impact of the vertical pushing force to cause floating instability remains same as per past descriptions and assumptions due to sub-critical state of the flow.

5.1.1 Rolling Resistance (F_{RO})

The rolling friction is even smaller than sliding friction and is considered trivial as the interlocking between the two surfaces is minimum in this case. This happens as the point of interaction of the tire with the surface changes all the time, and the friction is applied only at the smaller area of contact. Therefore, when a tire rolls forward in the clockwise direction, the resistive force in the opposite direction keeps the tire in contact with the ground. Basically, there are two primary mechanisms responsible for the friction between the tire and the road, as shown in Figure 20 [48]. The intermolecular force between the aggregate and the rubber on the road surface is caused by surface adhesion, which decreases when the surface is wet, causing the loss of friction, whereas the hysteresis mechanism represents the energy loss in the rubber as it deforms when sliding over the aggregate on the road. It is the difference between the amount of energy that is absorbed when a rubber object is stretched and the amount of energy released when the rubber object returns to its original shape. However, hysteresis friction is not so affected by water on the road surface [49].

5.1.1.1 Parameters Determination for Rolling Resistance

Rolling resistance can be simply defined as the energy a tire consumes while rolling under a given load. The resistance is influenced by the friction between the tire tread and the road surface, and the amount of energy consumed by the flexing of the tire sidewalls as the tire rolls over the road as shown in Figure 21 [50]. This scenario has been elaborated further by summing up all forces and dimensions separately into two different triangles, as shown in Figure 22. From the force perspective, F_{RO} is the force required to keep the wheel rolling, W is the weight of the load, R is the reactionary force and $\emptyset$ is the angle which relates to these three factors, whereas from the pure dimensions point of view, r is the radius of the wheel and b is the rolling coefficient which is measured in distance [51].

Thus, it can be said that:

$$R \sin \emptyset = F_{RO} \tag{55}$$

where, R is the reaction force caused by the friction force, $\emptyset$ is the angle and F_{RO} is the force required to keep the tire rolling. Following the concept of small-angle approximation it can be said that $\sin\emptyset = \tan\emptyset = \emptyset$ therefore, Eq. (55) can be written as:

$$R\emptyset = F_{RO} \tag{56}$$

Multiply Eq. (56) by the radius of the tire gives:

$$\frac{R\emptyset r}{r} = F_{RO} \tag{57}$$

From the pure dimensions point of view, it can be seen that $\sin \emptyset = \frac{b}{r}$, since $\sin\emptyset = \emptyset$ therefore, $\emptyset r = b$. So, substituting the value of $\emptyset r$ in Eq. (57) gives:

$$Rb = F_{RO}\, r \tag{58}$$

Using the Pythagoras theorem, it can be written as:

$$R = \sqrt{W^2 + F_{RO}^2} \tag{59}$$

Squaring Eq. (58) both sides gives:

$$R^2 b^2 = F_{RO}^2\, r^2 \tag{60}$$

Putting the value of R from Eq. (59) into Eq. (60), then Eq. (60) can be re-written as:

$$F_{RO} = \frac{Wb}{\sqrt{r^2 - b^2}} \tag{61}$$

For vehicles in floodwater (sub-critical conditions), Eq. (61) can be re-written as:

$$F_{RO} = \frac{(W - F_B)xb}{\sqrt{r^2 - b^2}} \tag{62}$$

where, F_{RO} is the resistive force required to keep the tire rolling, W is the weight of the load, F_B is the buoyancy force, b is the distance from the middle of the centre of the axle toward the tire no longer touching the ground, and r is the radius of the tire [51].

The coefficient of rolling resistance can also be determined experimentally by following a method similar to one proposed by Bonham and Hattersley (1967) and Gordan and Stone (1973) earlier. The horizontal force required by the tires to rotate can be estimated by using a spring balance manually. This force when divided by the scaled model weight estimates the coefficient of rolling friction. The resistive force to keep the tires rolling can also be given as:

$$F_{RO} = \mu_{RO}.F_G \tag{63}$$

where, μ_{RO} is the coefficient of rolling friction and F_G is the net weight of the vehicle. Therefore, it can be said:

$$F_{RO} = \frac{(W - F_B)xb}{\sqrt{r^2 - b^2}} = \mu_{RO}.F_G \tag{64}$$

5.1.2 Driving Force (F_{DV})

The car engine provides a driving force when it just begins to move; this driving force is greater than the opposing force on the wheels. Therefore, the vehicle accelerates in the direction of the resultant force. Once moving, the vehicles pushes the air out of the way, which exerts a force on the car opposite to its direction. This force is called air resistance, which increases as the speed of the car increases [53]. In the current investigation, the impact of air resistance has been neglected due to the low vehicle speed, but only the impact of drag force caused by floodwater has been taken into consideration. However, the driving force (F_{DV}) caused by vehicle engine can be given as:

$$F_{DV} = ma \tag{65}$$

where, m is the mass of the vehicle and a is the average acceleration which can be given as:

$$a = \frac{v_f - v_o}{t} \tag{66}$$

where, v_f is the final velocity, v_o is the initial velocity, and t is the time taken by the initial velocity to reach final velocity. For vehicles moving at constant velocity in water, the net force acting on them becomes zero; thus, the influence of driving force becomes negligible in that case. On flat roadways (dry conditions), the normal reaction force is equivalent to vehicle weight which can be written as:

$$F_N = W = mg \tag{67}$$

$$m = \frac{F_N}{g} \tag{68}$$

For the studies being performed in water, the net weight of the vehicle is equivalent to the vehicle weight in dry conditions minus the vertical pushing forces. However, for sub-critical flow states, the net weight of the vehicle can be given as:

$$F_N = W - F_B \tag{69}$$

Substituting Eq. (69) into Eq. (68) gives:

$$m = \frac{W - F_B}{g} \tag{70}$$

Substituting Eq. (70) into Eq. (65) gives:

$$F_{DV} = \left(\frac{W - F_B}{g}\right) x\ a \tag{71}$$

where, W is vehicle weight in dry conditions, F_B is the buoyancy force, g is the acceleration due to gravity and a is vehicle acceleration.

5.2 Incipient Velocity Formula for Moving Vehicle

The criterion of vehicle instability for a moving vehicle in floodwater differs from the stationary vehicle (brakes applied). This happens due to two main factors, namely resistive and driving force. In case a vehicle moves in the opposite way, parallel to the flow direction, then the resistive force is governed only by rolling friction. Conversely, the resistive force would be governed both by frictional force and rolling friction if a vehicle moves perpendicular to the flow direction, as highlighted in Figure 23. In the current study, the proposed incipient velocity formula has been derived based on the second assumption. Moreover, for the convenience of analysis, the instability thresholds of a non-stationary, partially submerged vehicle have only been proposed under the sub-critical flow conditions. Under such conditions, as the non-stationary vehicle starts to slide along a road surface, the drag force induced by the incoming flow is balanced by the frictional force and the driving force caused by the vehicle engine. Thus, the corresponding criterion of instability threshold can be given by:

$$F_D = F_{RO} + F_R + F_{DV} \tag{72}$$

By substituting the values of F_D (Eq. 4), F_{RO} (Eq. 62), F_R (Eq. 1) and F_{DV} (Eq. 65) into Eq. (72), the final proposed equation becomes:

$$\frac{1}{2}\rho C_D A_D v^2 = \frac{(W - F_b) \times b}{\sqrt{(r+b)(r-b)}} + (F_g - F_B)\ x\ \mu + ma \tag{73}$$

Rearrangement of Eq. (73) gives:

$$v = \sqrt{2 \times \frac{(W - \rho g V) x b + \{(F_g - \rho g V) x \mu + ma\}.\sqrt{(r+b)(r-b)}}{\sqrt{(r+b)(r-b)} \times \rho C_D A_D}} \tag{74}$$

where, v is the incipient velocity formula, W or F_g is the weight of vehicle in dry condition, ρ is the density of water, g is the acceleration due to gravity, V is the submerged volume of the vehicle, μ is the coefficient of frictional resistance on the tires side, m is the mass of the vehicle in floodwater which is equivalent to $\frac{W - F_B}{g}$, a is the average acceleration, r is the radius of the tire, b is the distance from the middle of the centre of the axle toward the tire no longer touching the ground, C_D is the drag coefficient for the partially submerged vehicle, and A_D is the submerged area of the vehicle projected normal to the flow. To strengthen Eq. (74), a validation graph is included comparing the experimental works (of the author's) on a moving vehicle, as shown in Figure 24. Details of this work, however, are not presented here. Interested readers should refer to the work of the authors on vehicle instability, vehicle in motion, floods and partial submergence which is available online [54].

6.0 Conclusions

This paper summarizes the literature on the stability of vehicles exposed to floodwaters by comparing different eras in time *i.e.* past, present and future. From the available analytical and experimental data, it appeared that almost all studies were solely dedicated to stationary (parked) vehicles, indicating the need for this research. Furthermore, the existing design guidelines on flood risk assessment were based on these assumptions and obeying to the depth-velocity domain criterion for stationary cars proposed in earlier studies. Due to the complexity of the stability analysis of vehicles in motion, the knowledge on non-stationary vehicles is still not well understood. Herein an incipient velocity formula for vehicles moving on a flat surface in floodwaters perpendicular to the direction of flow has been proposed for the very first time. For the convenience of the analysis, the instability thresholds of a partially submerged vehicle moving under the sub-critical flow condition was proposed. Since the mechanics of a moving vehicle under the influence of hydrodynamic forces differs from a stationary vehicle, assessing stabilities for the two should not be assumed to be the same. This includes the speed of the car, which imposes another unique force, namely acceleration and the rolling frictional resistance in the driving direction. The corresponding measured velocities (visually observed) agreed well with the predicted velocities using the proposed formula resulting in a reliable confidence of the incipient velocity. However, to ensure the practical application of the derived formula, a reliable assessment of drag and lift coefficients contributing to the incipient motion condition under different flow regimes needs to be conducted. Though today's computing capacities can carry out 3-dimensional numeric simulations on the drag and lift contribution to the incipient motion of partly submerged flooded vehicles, such studies are limited. More investigation of the force coefficients both for partial and full submergence is needed. To the author's knowledge, the assessment of lift coefficient, C_L and drag coefficient, C_D has only been undertaken for partly submerged vehicles where these coefficients were studied for different flow regimes. Despite that, the evaluation of C_L relies on the Froude number, which reflects the different pressure distributions on the vehicle. On the other hand, the value of C_D depends on the Reynolds number and the shape of the vehicle which varies with the level of vehicle submergence. Under full submergence, the drag coefficient is assessed as being that corresponding to a rectangular prism, whereas under partial submergence the wheels as well as some part of the chassis contributes to the drag force. However, it has been noticed that the evaluation of both C_D and C_L has not been quantified well both for fully and partially submerged vehicles and there is still a need for the reliable assessment of such coefficients.

Acknowledgement

This study was undertaken at Universiti Teknologi PETRONAS, Malaysia. This research was supported by Universiti Teknologi PETRONAS (UTP) Internal Grant URIF 0153AA-G24 and the Technology Innovation Program (Grant No.: 10053121) funded by the Ministry of Trade, Industry & Energy (MI, Korea). The authors would also like to thank for the great support of POSTECH, Republic of Korea.

References

1. Smith, G., 2015. Expert opinion: Stability of people, vehicles and buildings in flood water. *Water Research Laboratory, Technical Report 2015/11*. University of New South Wales. Sydney, Australia.
2. Shah, S.M.H., Mustaffa, Z., and Yusof, K.W., 2017. Disasters worldwide and floods in the malaysian region: a brief review. *Indian Journal of Science and Technology*, 10(2). doi: 10.17485/ijst/2017/v10i2/110385
3. Martínez-Gomariz, E., Gómez, M., Russo, B., and Djordjevic´, S., 2018. Stability criteria for flooded vehicles: a state-of-the-art review. *Journal of Flood Risk Management*, 11(S2), S817-S826. doi: 10.1111/jfr3.12262
4. Mok, O., 2017. Vehicles stuck in the flood at jalan air itam in george town - penang. http://media.themalaymailonline.com/print/malaysia/flash-floods-hit-penang-rivers-at-dangerous-level. Source: Malaymailonline
5. Versini, P.-A., Gaume, E., and Andrieu, H., 2010. Assessment of the susceptibility of roads to flooding based on geographical information–test in a flash flood prone area (the Gard region, France). *Natural Hazards and Earth System Sciences*, 10(4), 793-803.
6. Shu, C., Xia, J., Falconer, R.A., and Lin, B., 2011. Incipient velocity for partially submerged vehicles in floodwaters. *Journal of Hydraulic Research*, 49(6), 709-717.
7. Karnopp, D., 2004. Vehicle stability. *Marcel Dekker, Inc.* University of California. ISBN: 0-8247-5711-4. [google books]
8. Hammond, M.J., Chen, A.S., Djordjevic´, S., Butler, D., and Mark, O., 2015. Urban flood impact assessment: a state-of-the-art review. *Urban Water Journal*, 12(1), 14-29.
9. Sanyal, J. and Lu, X.X., 2006. GIS-based flood hazard mapping at different administrative scales: a case study in gangetic west bengal, india. *Singapore Journal of Tropical Geography*, 27(2), 207-220.
10. Vandrie, R., Simon, M., and Schymitzek, I., 2008. HAZARD:-Is there a better definition? & Impact of Not accounting for buildings!. *48th Annual Floodplain Management Authorities Conference*.
11. Russo, B., Velasco, M., and Suñer, D., 2013. Flood hazard assessment considering climate change impacts-application to barcelona case study using a 1D/2D detailed coupled model. *International Conference on Flood Resilience: Experiences in Asia and Europe*.
12. Abt, S.R., Wittier, R.J., Taylor, A., and Love, D.J., 1989. Human stability in a high flood hazard zone. *Journal of the American Water Resources Association*. 25(4), 881-890.
13. Russo, B., Gómez, M., and Macchione, F., 2013. Pedestrian hazard criteria for flooded urban areas. *Natural Hazards*. 69(1), 251-265.
14. Xia, J., Falconer, R.A, Wang, Y., and Xiao, X., 2014. New criterion for the stability of a human body in floodwaters. *Journal of Hydraulic Research*. 52(1), 93-104.
15. Shand, T.D., Cox, R.J., Blacka, M.J., and Smith, G.P., 2011. Appropriate safety criteria for vehicles. *Australian Rainfall and Runoff, P10/S2/020*. ISBN:978-0-85825-948-5.

16. Arrighi, C., Castelli, F., and Oumeraci, H., 2016. Effects of flow orientation on the onset of motion of flooded vehicles. *Sustainable Hydraulics in the Era of Global Change*. 837-841. doi: 10.1201/b21902-140
17. Persson, B.N.J, 2000. Sliding friction - physical principles and applications. *International Journal for Numerical and Analytical Methods in Geomechanics*. 24(1), 95-96.
18. Teo, F.Y., Xia, J., Falconer, R.A., and Lin, B., 2012. Experimental studies on the interaction between vehicles and floodplain flows. *International Journal of River Basin Management*. 10(2), 149-160.
19. Teo, F.Y., Falconer, R.A., Lin, B., and Xia, J., 2012. Investigations of hazard risks relating to vehicles moving in flood. *The Journal of Water Resources Management*. 1(1), 52-66.
20. Waters, S., 2016. Forces on vehicles crossing streams. *National Weather Service*. US Department of Commerce. http://nws.noaa.gov/os/water/tadd/pdfs/WaterPhysics.pdf
21. Young, D.F., Munson, B.R., Okiishi, T.H., and Huebsch, W.W., 2010. A brief introduction to fluid mechanics. *John Wiley & Sons*. ISBN: 13 978-0470-59679-1. [google books]
22. Poirot, S., 2012. Handbook of fluid dynamics and fluid hydronomics. *Auris Reference Ltd*. United Kingdom
23. Martínez-Gomariz, E., Gómez, M., Russo, B., and Djordjevic´, S., 2017. A new experiments-based methodology to define the stability threshold for any vehicle exposed to flooding. *Urban Water Journal*. 1-10. doi: 10.1080/1573062X.2017.1301501
24. Arrighi, C., Alcèrreca-Huerta, J.C., Oumeraci, H., and Castelli, F., 2015. Drag and lift contribution to the incipient motion of partly submerged flooded vehicles. *Journal of Fluids and Structures*. 57, 170-184.
25. Chien, N. and Wan, z., 1999. Mechanics of sediment transport. *American Society of Civil Engineers Press*. ISBN: 9780784478905.
26. Hall, N., 2015. The lift equation. *National Aeronautics and Space Administration*. https://www.grc.nasa.gov/www/k-12/airplane/lifteq.html
27. Xia, J., Teo, F.Y., Lin, B., and Falconer, R.A., 2011. Formula of incipient velocity for flooded vehicles. *Natural Hazards*. 58(1), 1-14.
28. Bettes, W.H., 1982. The Aerodynamic drag of road vehicles - past, present, and future. *Engineering and Science*. 45(3), 4-10.
29. Lajos, T., 2002. Basics of vehicle aerodynamics. *Budapest University of Technology and Economics, Department of Fluid Mechanics*.
30. Teo, F.Y., 2010. Study of the hydrodynamic processes of rivers and floodplains with obstructions. *Ph.D. Thesis*. https://orca.cf.ac.uk/54161/1/U517543.pdf
31. Smith, G.P., Modra, B.D., Tucker, T.A., and Cox, R.J., 2017. Vehicle stability testing for flood flows. *Water Research Laboratory, School of Civil and Environmental Engineering, Technical Report 2017/07*. University of New South Wales, Australia.
32. Arrighi, C., Huybrechts, N., Ouahsine, A., Chassé, P., Oumeraci, H., and Castelli, F., 2016. Vehicles instability criteria for flood risk assessment of a street network. *Proceedings of the International Association of Hydrological Sciences*. 373, 143-146. doi:10.5194/piahs-373-143-2016
33. Bonham, A.J., and Hattersley R.T., 1967. Low level causeways. *Water Research Laboratory, Report no. 100*. University of New South Wales, Australia.
34. Shand, T.D., Smith, G.P., Cox, R.J., and Blacka, M., 2011. Development of appropriate criteria for the safety and Stability of persons and vehicles in floods.

Proceedings of 34th International Association for Hydro-Environment Research and Engineering Congress.
35. Kramer, M., Terheiden, K., and Wieprecht, S., 2016. Safety criteria for the trafficability of inundated roads in urban floodings. *International Journal of Disaster Risk Reduction.* 17, 77-84.
36. Gordon, A.D, and Stone, P.B, 1973. Car stability on road floodways. *National Capital Development Commission, Report no. 73/12.* Water Research Laboratory, University of New South Wales, Australia.
37. Walsh, M., Benning, N., and Bewsher, D., 1998. Defining flood hazard in urban environments. *New South Wales, Department of Land and Water Conservation.* http://bewsher.com.au/techpapers.html
38. Wallingford, H.R., 2006. Flood risks to people: Phase 2. *Flood Hazard Research Centre, Report no. FD2321/TR2.* Middlesex University Risk & Policy Analysts Ltd.
39. Keller, R.J. and Mitsch, B., 1993. Safety aspects of the design of roadways as floodways. *Urban Water Research Association of Australia.* ISBN: 1875298703.
40. Yandell, W.O., 1973. Report on the coefficient of road-tyre friction under stationary flooded conditions of roads in Canberra. *Highway Engineering Note No 40, 7p.*
41. Woods, K.B., Berry, D.S., and Goetz, W.H., 1960. Highway engineering handbook. *New York: McGraw-Hill.*
42. Toda, K., Ishigaki, T., and Ozaki, T., 2013. Experiments study on floating car in flooding. *International Conference on Flood Resilience: Experiences in Asia and Europe.*
43. Xia, J., Falconer, R.A., Xiao, X., and Wang, Y., 2014. Criterion of vehicle stability in floodwaters based on theoretical and experimental studies. *Natural Hazards.* 70(2), 1619-1630.
44. Gerard, M., 2006. Tire-road friction estimation using slip-based observers. *Department of Automatic Control Lund University, MSc Thesis.* ISSN 0280-5316
45. Oshikawa, H., and Komatsu, T., 2014. Study on the risk evaluation for a vehicular traffic in a flood situation. *Proceedings of the 19th IAHR-APD Congress, Hanoi, Vietnam.*
46. Pregnolato, M., Ford, A., Wilkinson, S.M., and Dawson, R.J., 2017. The impact of flooding on road transport: a depth-disruption function. *Transportation Research Part D: Transport and Environment.* 55, 67-81.
47. Xia, J., Teo, F.Y., Falconer, R.A., Chen, Q., and Deng, S., 2018. Hydrodynamic experiments on the impacts of vehicle blockages at bridges. *Journal of Flood Risk Management.* 11(S1), S395-S402
48. Meyer, W.E., and Kummer, H.W., 1962. Mechanism of force transmission between tire and road. SAE Technical Paper. doi: https://doi.org/10.4271/620407
49. Gillespie, T.D., 1992. Fundamentals of vehicle dynamics. Society of Automotive Engineers, Inc. [google books]
50. Ejsmont, J.A., Ronowski, G., Świeczko-Żurek, B., and Sommer, S., 2017. Road texture influence on tyre rolling resistance. *Road Materials and Pavement Design.* 18(1), 181-198. doi: https://doi.org/10.1080/14680629.2016.1160835
51. Biezen, M.V., 2017. What is rolling fricition. *Ch 11: Friction, Mechanical Engineering.* http://ilectureonline.com
52. Wilson, D., 2017. Tire rolling resistance. https://www.tirebuyer.com
53. Royston, A., 2013. Forces and motion. *Heinemann Educational Books.* [google books]
54. Shah, S.M.H., Mustaffa, Z., Yusof, K.W., and Kim, D.K., 2018. Instability criteria for vehicles in motion exposed to flood risks. *MATEC Web of Conferences.* Article number 070032018, code 140464, vol 203. doi: 10.1051/matecconf/201820307003

Figure 1: Flooded vehicles in the 2017 George Town, Penang (Malaysia) flood [4].

Figure 2: Forces on a stationary vehicle in floodwaters.

Figure 3: Modes of vehicle instability [15].

Figure 4: Model Ford Falcon at 1:25 scale used by Bonham and Hattersley (1967) [33].

Figure 5: Raw test results of Bonham and Hattersley (1967) with the calculated coefficient of friction required to initiate sliding indicated and their assessed lines of constant friction indicated [15].

Figure 6: Morris Mini (1:16) for model testing undertaken by Gordon and Stone (1973) [15].

Figure 7(a): Raw test results of Gordon and Stone (1973) with the observed horizontal forces and front wheels' vertical reaction forces [15].

Figure 7(b): Raw test results of Gordon and Stone (1973) with the observed horizontal forces and rear wheels' vertical reaction forces [15].

Figure 8(a): Theoretical results assessed by Keller and Mitsch (1993) for a range of vehicle types assuming drag coefficient of 1.1 and 1.15 and a frictional coefficient of 0.3 [15].

Figure 8(b): The limiting Dxv values assessed by Keller and Mitsch (1993) for a range of vehicle types assuming drag coefficient of 1.1 and 1.15 and a frictional coefficient of 0.3 [15].

Figure 9: Flume views (a)Smaller flume and (b)Wider flume.

Figure 10: Threshold values for model vehicles with rear end facing the flow.

Figure 11: Different vehicle orientations to the flow (a)Rear end of the vehicle facing the flow i.e. 0° (b) Side ends of the vehicle facing the flow i.e. 45°, 60° etc. (c) Vehicle positioned perpendicular to the flow direction i.e. 90°.

Figure 12: Partially submerged model vehicles in flume (a)Ford Focus positioned at 0° and (b)Ford Transit positioned at 0°.

Figure 13: Depth-incipient velocity relationships for partially submerged model vehicles (a) ford Focus, (b) Ford Transit and (c) Volvo Xc90.

Figure 14: Experimental Setup (a) Flume Description (b) Schematic Diagram.

Figure 15: Orientation angles i.e. 0°, 180°, and 90°.

Figure 16: Depth–incipient velocity relationships for large-scale model vehicles for different orientation angles.

Figure 17: Experimental setup.

Figure 18: Determination of friction coefficient.

Figure 19: Buoyancy test.

Figure 20: Mechanism of tire-road friction [48].

Figure 21: Tire rolling resistance [52].

Figure 22: Schematic diagram for forces and dimensions [51].

Figure 23: Forces on a non-stationary vehicle in floodwater.

Figure 24: Formula validation with experimental data.

Table 1: Summary of the earlier analytical and theoretical studies (adapted and modified from [15] (1 of 2).

Reference	**Bonham and Hattersley (1967)**	**Gordon and Stone (1973)**	**Keller and Mitsch (1993)**
Study Mode	Experimental	Experimental	Theoretical
Vehicles Tested	*Ford Falcon *Results Scaled to other models	*Morris Mini Sedan	*Toyota Corolla, *Suzuki Swift, *Ford Laser, *Honda Civic, *Ford LTD
Vehicle Age	Mid to late 1960s	Early 1970s	Early 1990s
Ground Clearance (m) – Prototype	0.18	0.15	0.155, 0.17, 0.15, 0.10, 0.16
Scale	1:25	1:16	-
Orientation	Perpendicular to flow	Parallel to flow	Perpendicular to flow
Submergence	Partial	Partial	Partial
Surface Type	-	-	-
Ground Slope	Flat	Flat	-
Range of depths tested (m) – Prototype	0.11 to 0.57	0.12 to 0.57	0.025 to 0.375
Range of velocities tested (m/s) – Prototype	0.48 to 3.09	0.5 to 3.69	0.6 to > 3.5
Buoyancy depth (m) - Prototype	0.57	0.42 (rear) and 0.5 (front)	Between 0.34 and 0.4 for different models
Resultant Equation of Stability	$\frac{F_H}{\mu F_v} = 1$	$\frac{F_H}{\mu F_v} = 1$	$v = 2 \times \left(\frac{\mu F_v}{\rho C_D A_D}\right)^{\frac{1}{2}}$
Assumed Coefficient of Friction	Various, recommended 0.3	Various, ranging between 0.3-1.0	0.3

Table 2. Summary of the recent analytical and theoretical studies (adapted and modified from [15] (2 of 2).

Reference	**Teo *et al.* (2010)**	**Xia *et al.* (2010)**	**Shu *et al.* (2011)**
Study Mode	Experimental	Theoretical	Experimental and Theoretical
Vehicles Tested	*Mini Cooper, *BMW M5 and *Mitsubishi Pajero	Validation of his derived formula based on Teo *et al.* (2010) experimental results	*Ford Focus, *Ford Transit and *Volvo XC90
Vehicle Age	Actuals	Actuals	Actuals
Ground Clearance (m) – Prototype	0.149; 0.177; 0.225	0.149; 0.177; 0.225	0.101; 0.166; 0.218
Scale	1:43 and 1:18	-	1:18
Orientation	Several orientations between 0° and 90°	Parallel to flow only (rear end facing the flow)	Parallel to flow i.e. 0° and 180° (both rear and front ends facing the flow)
Submergence	Both partial and full	Full	Partial
Surface Type	Rough bed surface	-	Wet carpet
Ground Slope	Flat	-	Flat
Range of depths tested (m) – Prototype	0.645 to 4.816	0.3 to 3.0	0.16 to 0.62
Range of velocities tested (m/s) – Prototype	2.37 to 7.94	0.5 to 4.0	0.18 to 6.24
Buoyancy depth (m) - Prototype	Not available	Not available	Not available
Resultant Equation of Stability	$U_c = \left[2\mu N/(\rho C_D A)\right]^{1/2}$ Being, μ: friction coefficient N: axle load in dry condition minus buoyancy ρ: water density C_D: drag coefficient A: submerged area projected normal to the flow	$U_c = \propto \times \left(\frac{y}{h_c}\right)^{\beta} \times \sqrt{2g\left(\frac{\rho_c - \rho_w}{\rho_w}\right)h_c}$ Being, α,β: empirical parameters for each vehicle y,h_c: water depth and vehicle height ρ_c, ρ_w: vehicle and water density	$U_c = \propto \times \left(\frac{y}{h_c}\right)^{\beta} \times \sqrt{2gl_c\left(\frac{\rho_c h_c}{\rho_w y} - \frac{h_c \rho_c}{h_b \rho_w}\right)}$ Being, α,β: empirical parameters for each vehicle y,h_c: water depth and vehicle height ρ_c, ρ_w: vehicle and water density h_b: buoyancy depth l_c: vehicle length
Assumed Coefficient of Friction	-	-	0.39 (Transit); 0.50 (Focus); 0.68 (Volvo)

Continued.

Reference	**Toda *et al.* (2013)**	**Xia *et al.* (2013)**	**Martínez-Gomariz *et al.* (2017)**
Study Mode	Experimental	Experimental and Theoretical	Experimental
Vehicles Tested	*Tipo Sedan and *Tipo Minivan	*Honda Accord and *Audi Q7	*BMW 650 (1:14), *Mini Cooper (1:18; 1:24 and 1:14), *BMW i3 (1:14), *Mercedes GLA (1:14), *Mercedes Clase C (1:18), *Range Rover Evoque (1:14), *Porsche Cayenne Turbo (1:14), *Bentley Continental GT Speed (1:18), *Volkswagen Touareg (1:14), *BMW X6 (1:14), *Audi Q7 (1:14) and *Mercedes G55 AMG (1:14)
Vehicle Age	Actuals	Actuals	Actuals
Ground Clearance (m) – Prototype	-	0.155; 0.206	0.084; 0.126; 0.120; 0.154; 0.154; 0.168; 0.162; 0.168; 0.182; 0.180; 0.224; 0.224; 0.252; 0.280
Scale	1:10 (Sedan); 1:18 (Minivan)	1:14 and 1:24	1:14; 1:18 and 1:24
Orientation	0°, 45° and 90°	0° and180° (Parallel to flow) 90° (Perpendicular to flow)	All

Submergence	Partial submergence	Partial submergence	Partial submergence
Surface Type	Mortar platform	Thin cement layer	Bakelite
Ground Slope	Flat	Flat, 1:50 and 1:100	Flat
Range of depths tested (m) – Prototype	0.30 to 0.69 (Sedan) 0.43 to 1.21 (Minivan)	0.18 to 0.55	0.4 to 0.68
Range of velocities tested (m/s) – Prototype	1.05 to 2.00 (Sedan) 1.24 to 2.35 (Minivan)	1.4 to 5.4	0.0 to 5.0
Buoyancy depth (m) - Prototype	Sedan-type cars likely to float based on the conditions: $U > 2.0$, $h > 0.5$ Being, U: flow velocity h: water depth	0.45 (Honda) 0.67 (Audi)	0.392; 0.387; 0.396; 0.399; 0.406; 0.434; 0.450; 0.462; 0.532; 0.531; 0.504; 0.595; 0.511; 0.686
Resultant Equation of Stability	$\frac{F_D}{\mu\,(M_c g - F_B - F_L)} = 1$ Being, μ: friction coefficient F_D: drag force M_c: vehicle weight F_B: buoyancy force F_L: lift force	Parallel $U_c = \propto \times \left(\frac{y}{h_c}\right)^{\beta} \times \sqrt{2gl_c\left(\frac{\rho_c h_c}{\rho_w y} - \frac{h_c \rho_c}{h_b \rho_w}\right)}$ Perpendicular $U_c = \propto \times \left(\frac{y}{h_c}\right)^{\beta} \times \sqrt{2gb_c\left(\frac{\rho_c h_c}{\rho_w y} - \frac{h_c \rho_c}{h_b \rho_w}\right)}$ Being, α,β: empirical parameters for each vehicle y,h_c: water depth and vehicle height ρ_c, ρ_w: vehicle and water density h_b: buoyancy depth l_c, b_c: vehicle length and width	$(v.y) = 0.0158.SC_{mod} + 0.32$ Being, (v.y): stability threshold for each vehicle SC_{mod}: modified stability coefficient $SC_{mod} = \frac{GC.M_c}{PA}.\mu$ Being, GC: ground clearance M_c: Kerb weight PA: plan areaμ: friction coefficient
Assumed Coefficient of Friction	Sedan (0°): 0.26 (hand brake), 0.073 (no hand brake) Sedan (90°): 0.565 (no hand brake) Minivan (0°): 0.42 (hand brake), 0.10 (no hand brake) Minivan (90°): 0.65 (no hand brake)	0.25 (parallel) 0.75 (perpendicular)	0.52 to 0.62

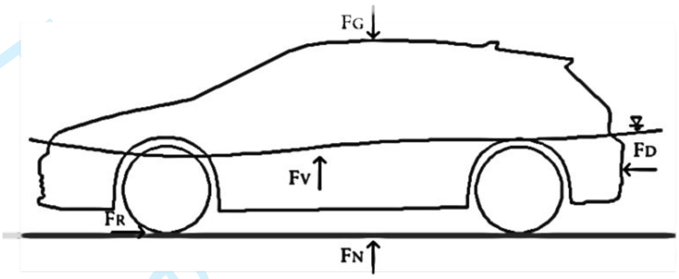
FG
FD
FV
FR
FN

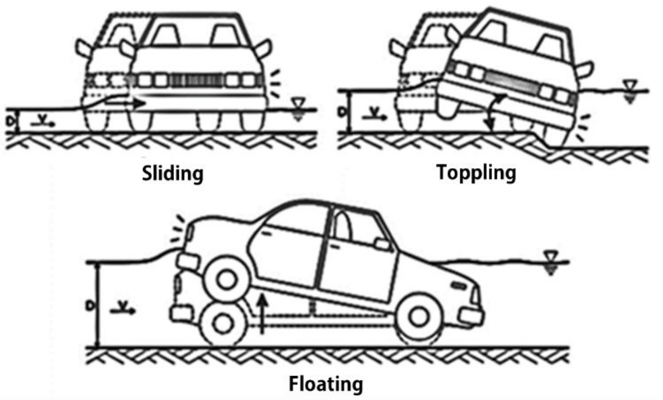
Sliding
Toppling
Floating

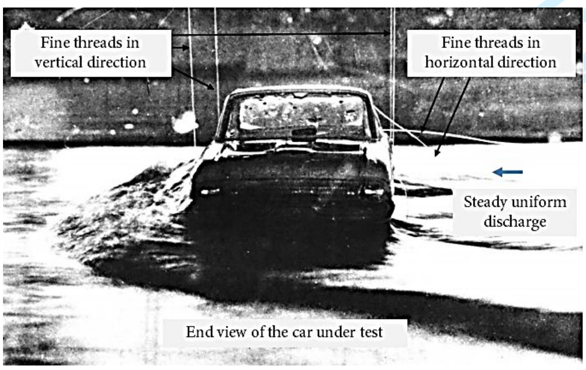
Fine threads in vertical direction
Fine threads in horizontal direction
Steady uniform discharge
End view of the car under test

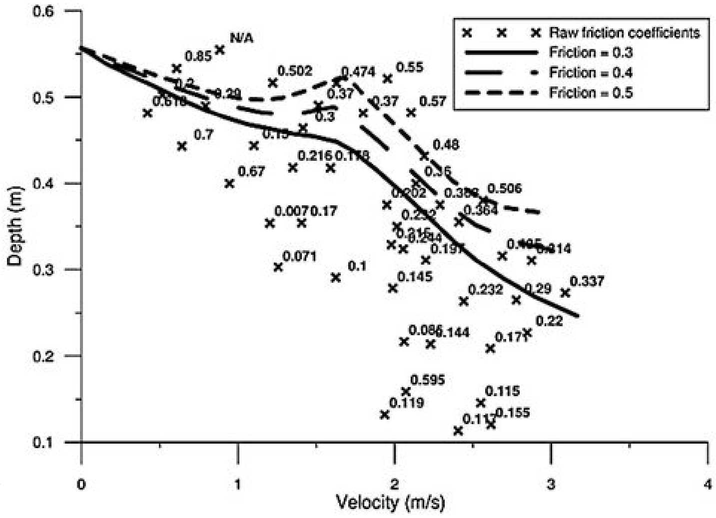
Raw friction coefficients
Friction = 0.3
Friction = 0.4
Friction = 0.5
Depth (m)
Velocity (m/s)

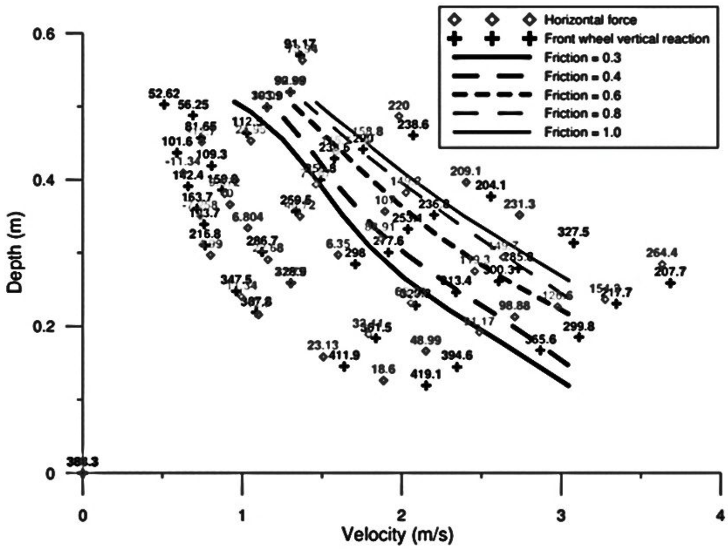
Horizontal force
Front wheel vertical reaction
Friction = 0.3
Friction = 0.4
Friction = 0.6
Friction = 0.8
Friction = 1.0
Depth (m)
Velocity (m/s)

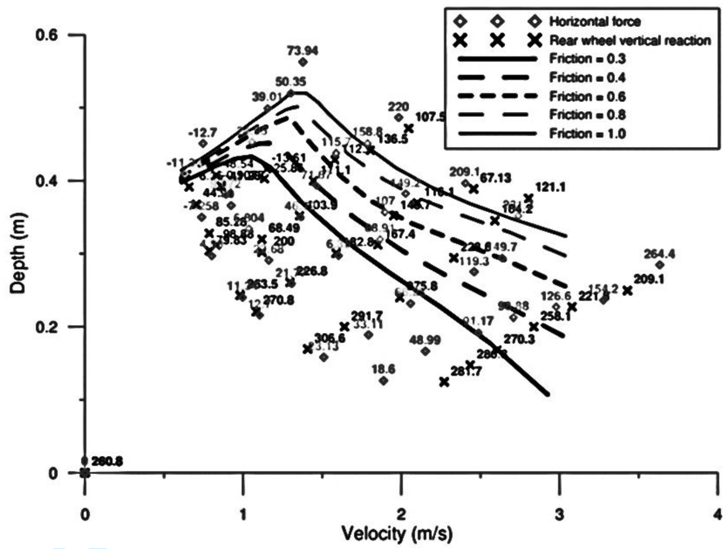
Horizontal force
Rear wheel vertical reaction
Friction = 0.3
Friction = 0.4
Friction = 0.6
Friction = 0.8
Friction = 1.0
Depth (m)
Velocity (m/s)

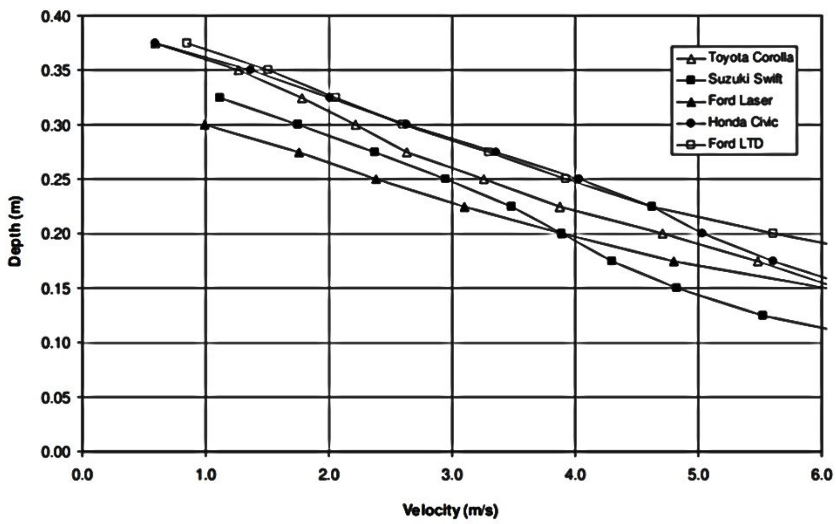
Toyota Corolla
Suzuki Swift
Ford Laser
Honda Civic
Ford LTD
Depth (m)
Velocity (m/s)

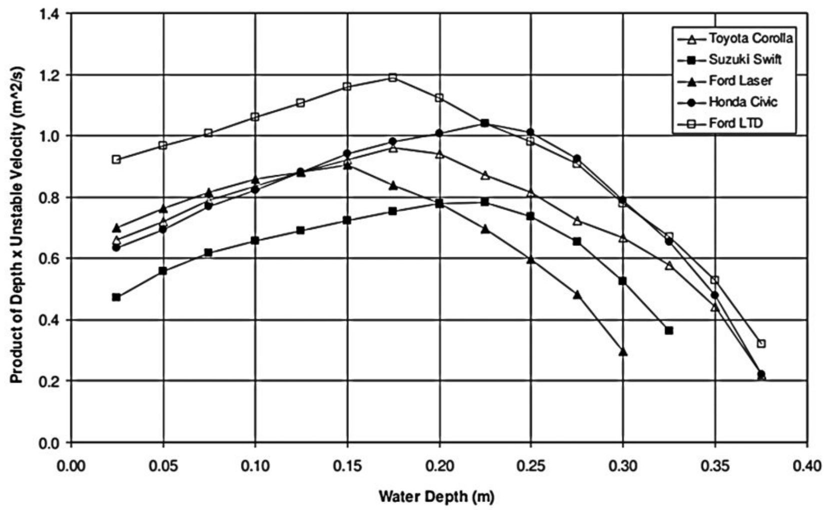
Toyota Corolla
Suzuki Swift
Ford Laser
Honda Civic
Ford LTD
Product of Depth x Unstable Velocity (m^2/s)
Water Depth (m)

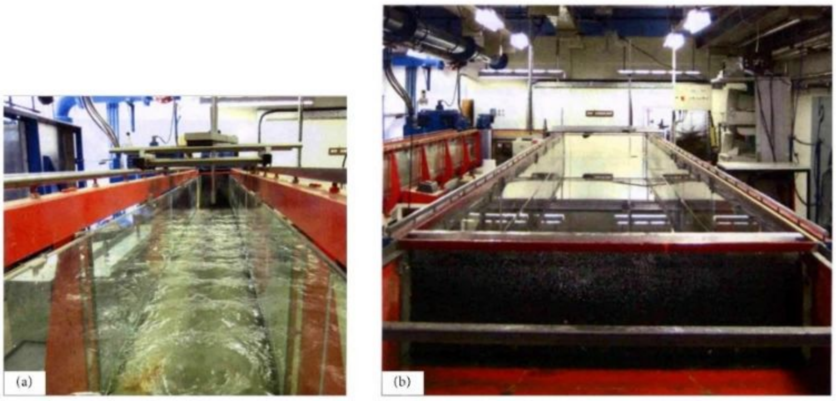
(a)
(b)

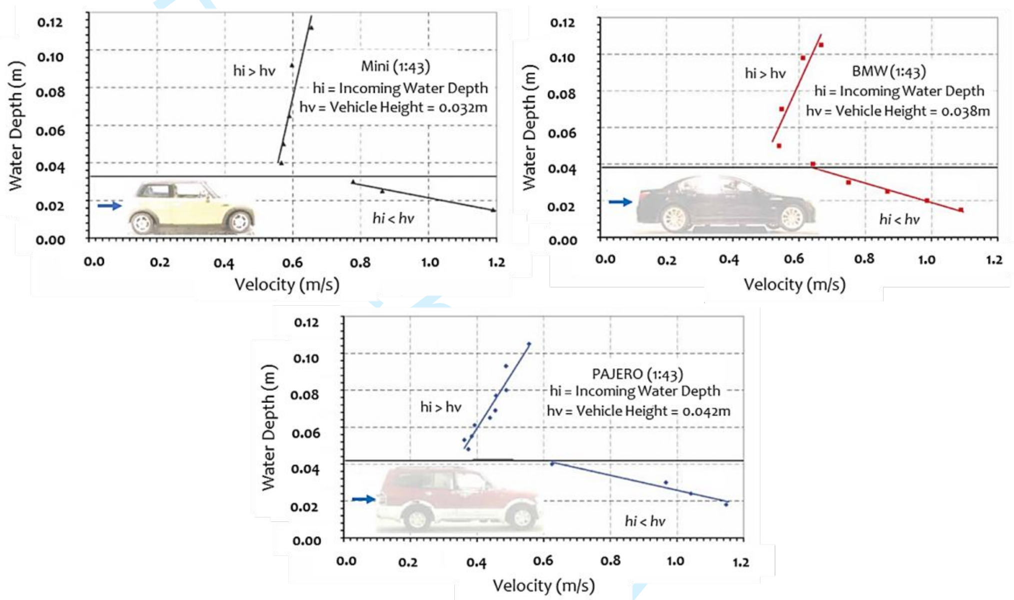
Mini (1:43)
hi = Incoming Water Depth
hv = Vehicle Height = 0.032m
hi > hv
hi < hv
Water Depth (m)
Velocity (m/s)
BMW (1:43)
hi = Incoming Water Depth
hv = Vehicle Height = 0.038m
hi > hv
hi < hv
Water Depth (m)
Velocity (m/s)
PAJERO (1:43)
hi = Incoming Water Depth
hv = Vehicle Height = 0.042m
hi > hv
hi < hv
Water Depth (m)
Velocity (m/s)

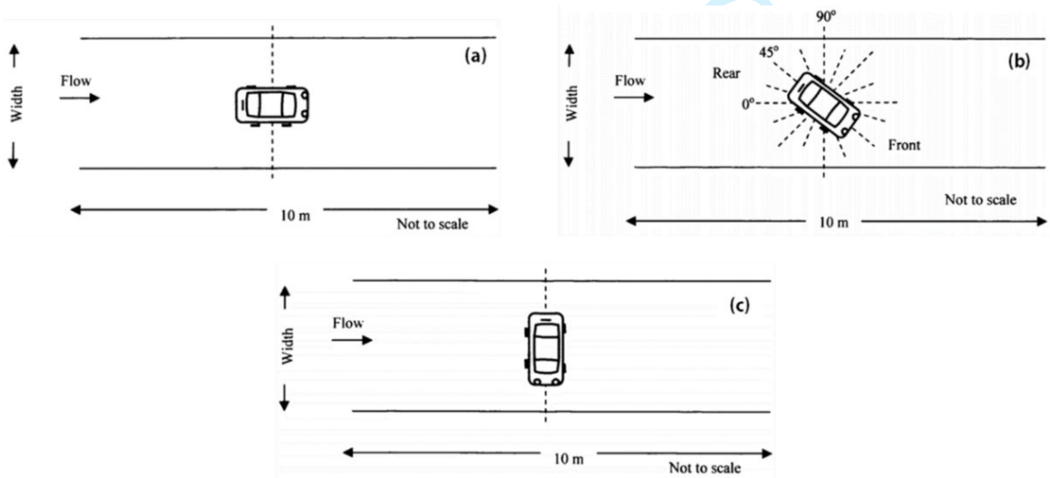
(a)
Flow
Width
10 m
Not to scale
(b)
90°
45°
Rear
0°
Front
Flow
Width
10 m
Not to scale
(c)
Flow
Width
10 m
Not to scale

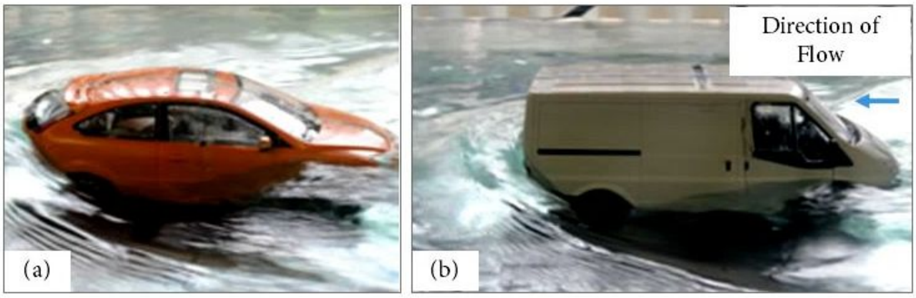
Direction of Flow
(a)
(b)

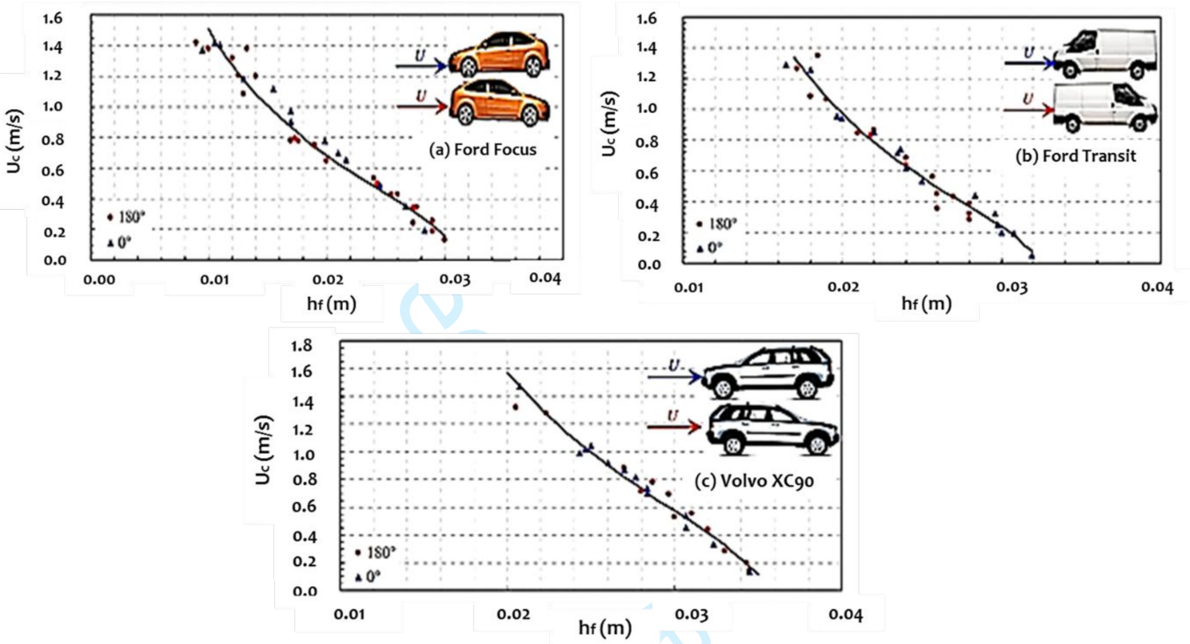
(a) Ford Focus
(b) Ford Transit
(c) Volvo XC90
Uc (m/s)
hf (m)
180°
0°

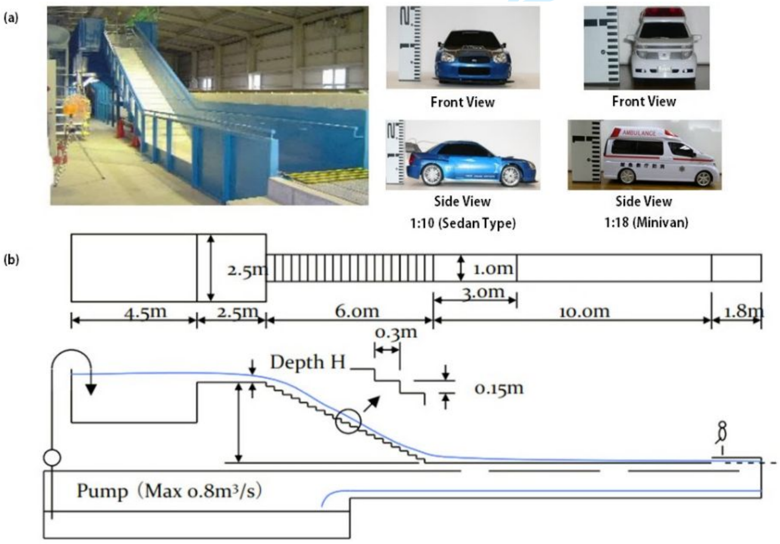
(a)
Front View
Front View
Side View
1:10 (Sedan Type)
Side View
1:18 (Minivan)
(b)
2.5m
1.0m
3.0m
4.5m
2.5m
6.0m
10.0m
1.8m
0.3m
Depth H
0.15m
Pump (Max 0.8m³/s)

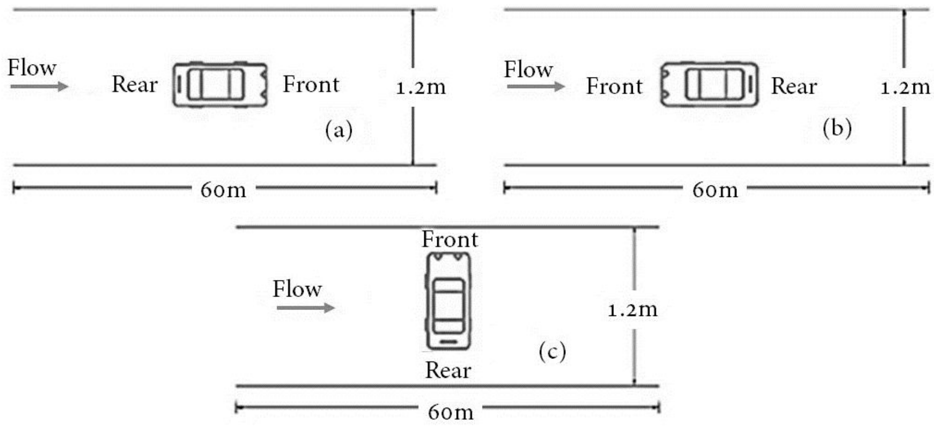
Flow
Rear
Front
1.2m
(a)
60m
Flow
Front
Rear
1.2m
(b)
60m
Front
Flow
1.2m
Rear
(c)
60m

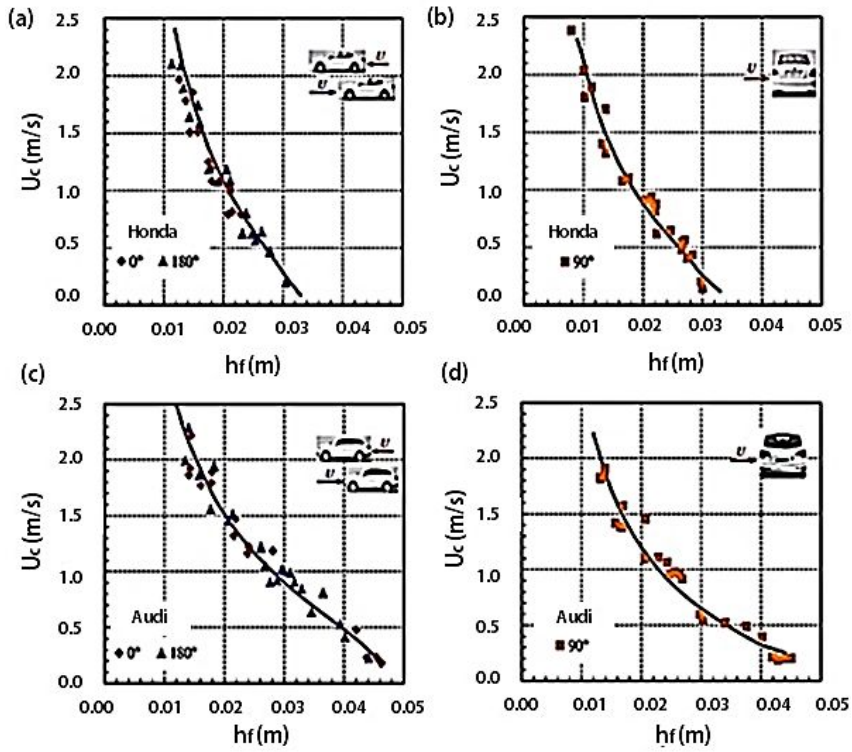
(a)
Uc (m/s)
Honda
0° 180°
hf (m)
(b)
Uc (m/s)
Honda
90°
hf (m)
(c)
Uc (m/s)
Audi
0° 180°
hf (m)
(d)
Uc (m/s)
Audi
90°
hf (m)

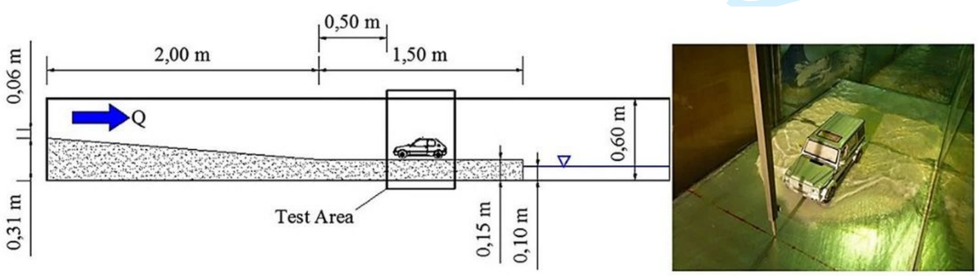
0,50 m
2,00 m
1,50 m
0,06 m
Q
0,60 m
0,31 m
Test Area
0,15 m
0,10 m

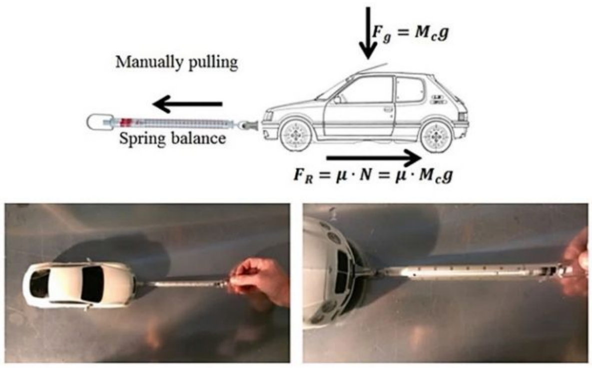
$F_g = M_c g$
Manually pulling
Spring balance
$F_R = \mu \cdot N = \mu \cdot M_c g$

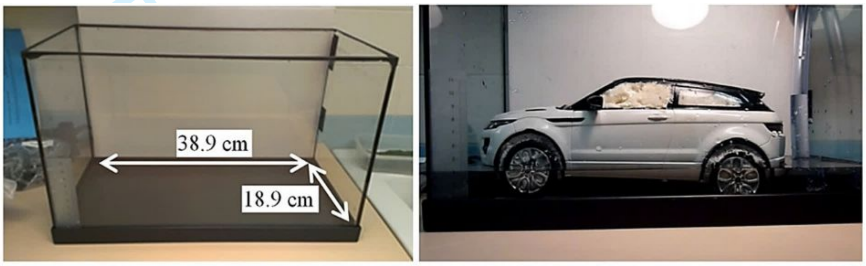
38.9 cm
18.9 cm

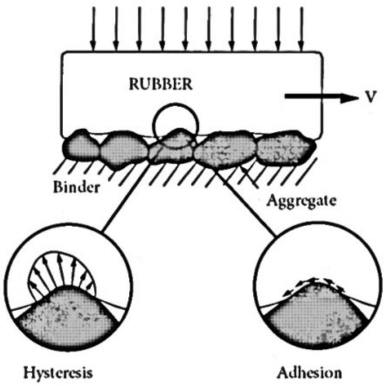
RUBBER
V
Binder
Aggregate
Hysteresis
Adhesion

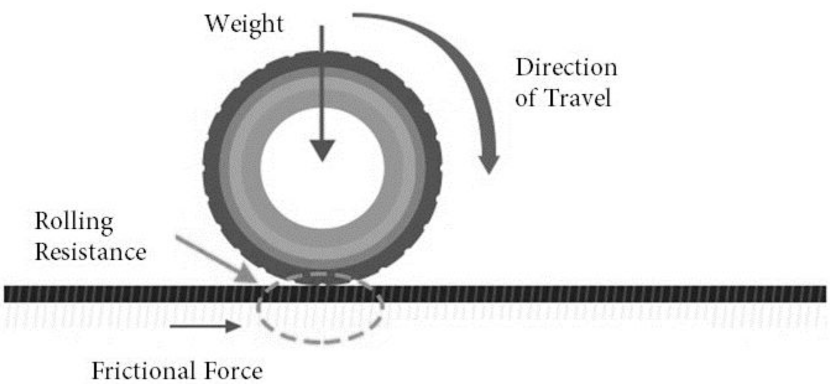
Weight
Direction
of Travel
Rolling
Resistance
Frictional Force

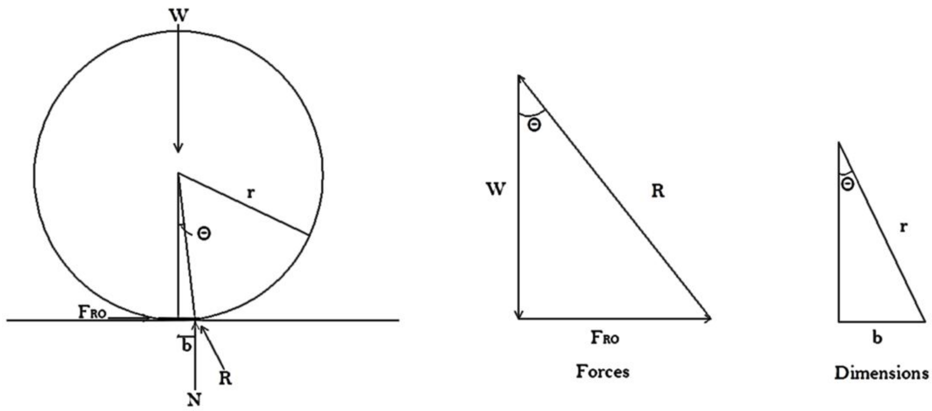
W
r
Θ
FRO
b
R
N
W
R
FRO
Forces
r
b
Dimensions

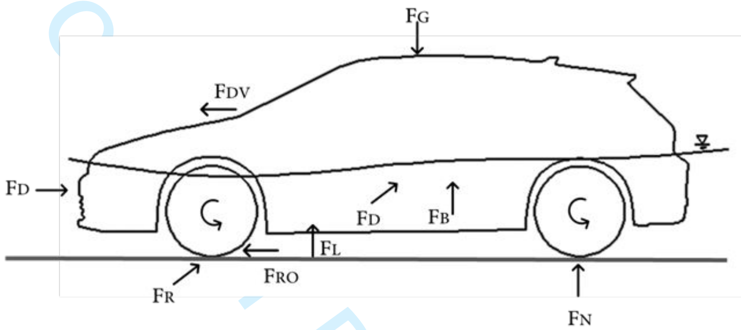
FG
FDV
FD
FD
FB
FL
FRO
FR
FN

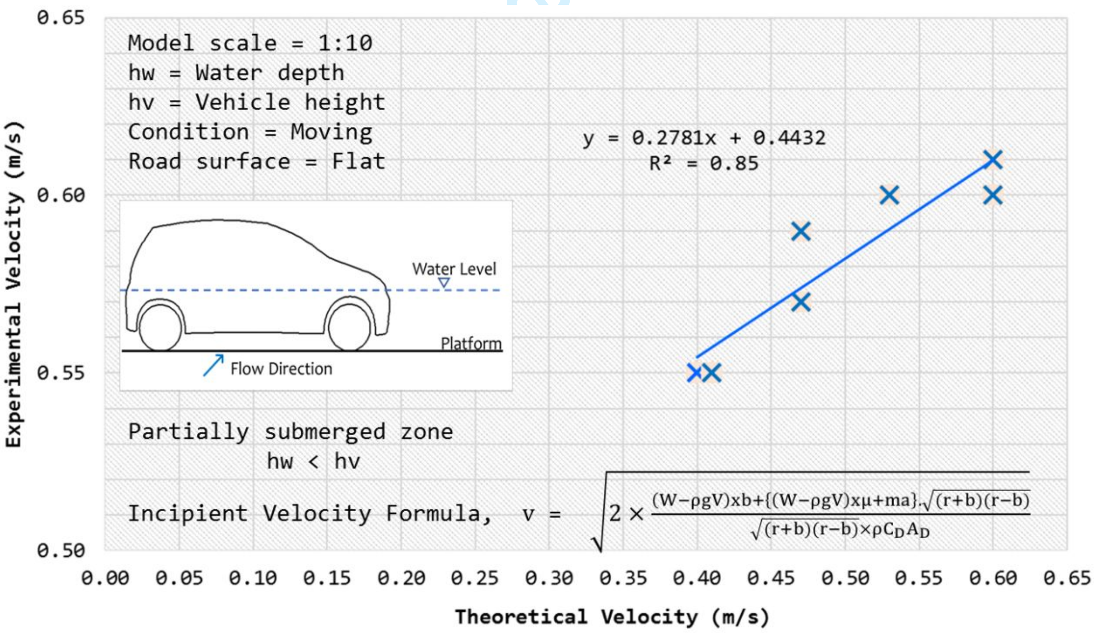
Model scale = 1:10
hw = Water depth
hv = Vehicle height
Condition = Moving
Road surface = Flat
y = 0.2781x + 0.4432
R² = 0.85
Water Level
Platform
Flow Direction
Partially submerged zone
hw < hv
Incipient Velocity Formula, v = √(2 × ((W−ρgV)xb+{(W−ρgV)xμ+ma}.√((r+b)(r−b))) / (√((r+b)(r−b))×ρCDAD))
Experimental Velocity (m/s)
Theoretical Velocity (m/s)
0.50
0.55
0.60
0.65
0.00 0.05 0.10 0.15 0.20 0.25 0.30 0.35 0.40 0.45 0.50 0.55 0.60 0.65